



OPEN ACCESS

EDITED BY Chengxi Zhang, Jiangnan University, China

Qi Wang. Northeast Agricultural University, China Hua Fei, Jiangnan University, China Beijing University of Technology, China

*CORRESPONDENCE Guogiang Dun, □ dunguoqiangpaper@163.com

RECEIVED 12 September 2025 REVISED 04 November 2025 ACCEPTED 05 November 2025 PUBLISHED 02 December 2025

CITATION

Dun G, Ma C, Zhang C, Ji X and He Y (2025) Optimization design and experiment of Chinese cabbage (Brassica rapa pekinensis) groovespoon type precision seed metering device based on discrete element method. Front. Mech. Eng. 11:1704283. doi: 10.3389/fmech.2025.1704283

© 2025 Dun, Ma, Zhang, Ji and He. This is an open-access article distributed under the terms of the Creative Commons Attribution License (CC BY). The use, distribution or reproduction in other forums is permitted, provided the original author(s) and the copyright owner(s) are credited and that the original publication in this journal is cited, in accordance with accepted academic practice. No use, distribution or reproduction is permitted which does not comply with these terms.

Optimization design and experiment of Chinese cabbage (Brassica rapa pekinensis) groove-spoon type precision seed metering device based on discrete element method

Guoqiang Dun^{1*}, Chunyu Ma², Chaoxia Zhang², Xinxin Ji² and Yang He²

¹Intelligent Agricultural Machinery Equipment Engineering Laboratory, Harbin Cambridge University, Harbin, China, ²College of Mechanical and Electrical Engineering, Northeast Forestry University, Harbin,

Aiming at problems such as Chinese cabbage seeds' small size, easy breakage, light quality, difficulty realizing single grain precision sowing, injury, and poor uniformity of seed discharge, a kind of groove-spoon type precision seed metering device with a guide ring combining a groove U-hole for Chinese cabbage was proposed. The seeding spoon features a tapered platform design, with a smaller upper section and a larger lower section. Preventing seed buildup during filling and enhancing single-seed sowing probability. It reduces seed damage caused by gravity-based seed clearance, incorporates seed guide rings and discharge channels to assist seed release, and improves seed distribution uniformity. The key structural parameters and working parameters of the seed metering device were determined through theoretical analysis, and the force analysis of cabbage seeds in filling, clearing, guiding, and casting was carried out. The discrete element single factor simulation test and quadratic regression orthogonal rotation combination test were conducted with U-hole diameter, U-hole depth, and inclination angle of the top of the seed scoop as test factors, and qualified rate, multiple rate and leakage rate as test indexes, the test results show that when the U-hole diameter is 2.32 mm, the U-hole depth is 1.76 mm. The inclination angle of the top of the seed spoon is 15.34°, and the seed metering device works optimally. Based on the simulation test, bench test, and field test under the optimal parameter combination, the results of the simulation test showed a qualified rate of 92.22%, a multiple rates of 4.21%, and a leakage rate of 3.57%; the qualified index of the bench test result 91.33%, the multiple indexes is 4.89%, and the leakage index is 3.78%, and the error value between the simulation and the bench test result is small, which proves the reliability of the simulation test; when the forward speed of the planter was 0.4-1.2 m/s, the qualified index of the field test was 89.90%, the multiple indexes was 6.06%, and the leakage index was 4.04%, which meets the planting requirements of Chinese cabbage precision direct seeding.

Chinese cabbage seed, groove-spoon type seed metering device, optimization design, discrete element simulation, high-speed photography

1 Introduction

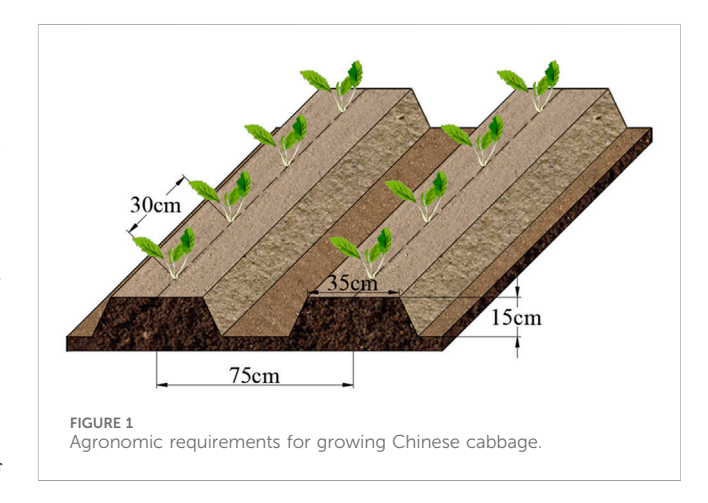
Chinese cabbage is a significant edible vegetable and traditional medicinal crop in China; it is abundant in vitamins, dietary fiber, and antioxidants and has a crucial role in the nutritional framework of Chinese residents. Chinese cabbage cultivation and market demand have grown in recent years. However, limited mechanization, high labor intensity associated with manual sowing, and high sowing costs have made it much harder to industrialize and grow cabbage on a large scale (Zhou and Qian, 2022; Yao, 2024). Consequently, it is vital to advance highly effective mechanized precision sowing apparatus for Chinese cabbage.

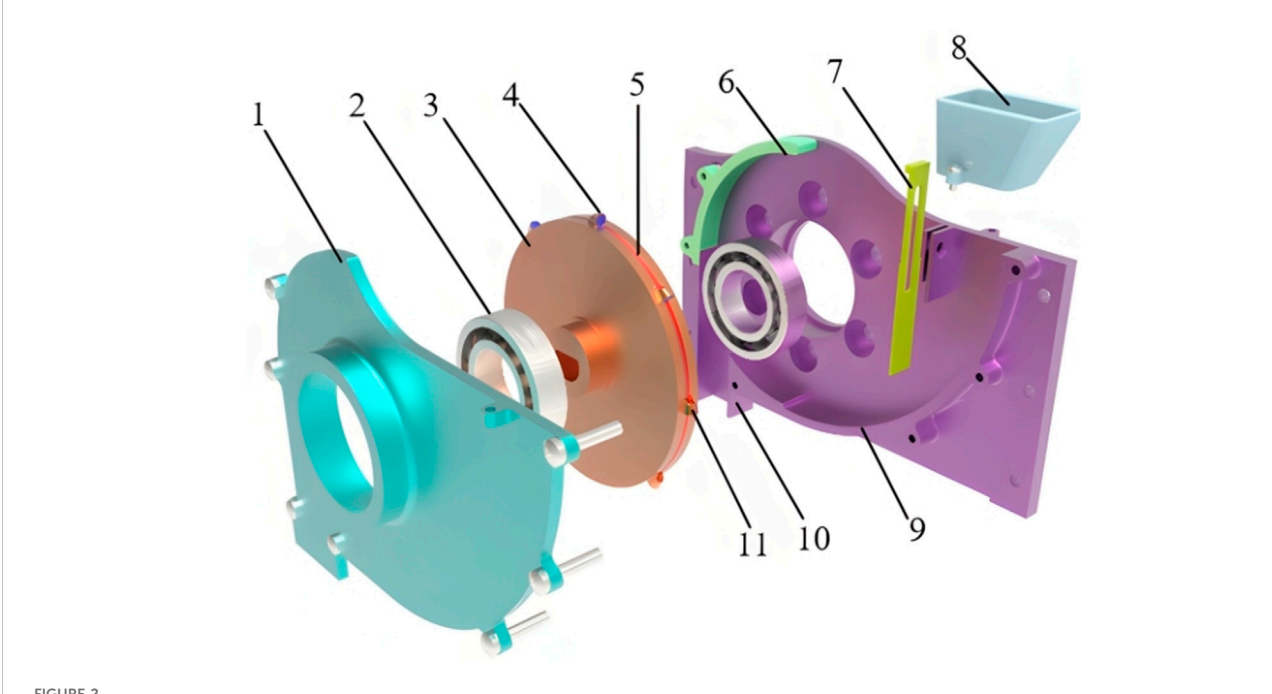
Accurate seed placement is a fundamental technical and agronomic prerequisite for the robotic sowing of Chinese cabbage. Currently, seed metering systems are primarily categorized into two types: pneumatic and mechanical, depending on their operational principles. Many people use seed metering devices instead of pneumatic seed metering devices because they are more reliable, cost less to make, and have a simpler design (Wang et al., 2024; Ma et al., 2024; Gao et al., 2021). The spoon-type seed metering device, a category of mechanical seed metering devices, offers features such as excellent seed-filling performance, straightforward single seed discharge, and robust adaptability. Researchers have examined numerous facets of it both domestically and internationally. A study by Zhang et al. (2023) improved the design of a spoon groove disc for spoon-type sorghum precision seed metering equipment. Field tests showed that the device was successful at 90.67% of the time for single-grain precision sowing. Su et al. (2022) Engineered a groove-spoon-type precision seed metering device for Chinese herbal medicine. Pinellia ternata fixes the problems that come with the uneven shape of Chinese herbal medicine seeds, which can cause the epidermal layer to tear, which stops the seeds from filling properly and damages them. Li et al. (2020) Designed a groove-spoon type garlic single-seed extraction device, compared and optimized the structural shapes of the seed spoon and seeding groove through discrete element simulation software, and determined the optimal structural parameter combinations of the seed spoon and seed extraction groove; Xu et al. (2019) used EDEM simulation software to carry out orthogonal simulation tests on the tilting disc scoop type soybean seed feeder, and established regression equations of qualified index and variation index in order to improve the seed stability and uniformity of the device; Chen et al. (2023) combined corn seed discrete element model with multiple nonlinear regression method by using discrete element method, optimized the performance of spoon-groove corn precision seed metering device, obtained the optimal parameter combination of the seed feeder, and finally verified by bench test, and the relative error between simulation results and bench test results was less than 5%. Extensive local and international studies on spoon seed metering systems indicate that they are mostly appropriate for large grain-size crops, including garlic, soybeans, and maize. Conversely, there has been limited study on spoon precision seed metering devices appropriate for small, fragile grain sizes. Consequently, high-quality crop seeds, such as Chinese cabbage, are essential for investigating a novel spoon seeder designed to fulfill the precision sowing requirements of Chinese cabbage and other particle seeds while leveraging the benefits of the spoon-type seed metering apparatus.

In order to realize the mechanized precision sowing of Chinese cabbage seeds, this paper combines the physical properties of Chinese cabbage seeds and the agronomic requirements of sowing to design a groove-spoon type precision Seed-metering device with a U-hole for Chinese cabbage that adopts gravity seed clearing and increases the guide ring groove and seed unloading groove to assist seed discharge. Firstly, the main factors affecting the seeddisplacing performance of the seed displacer and the range of their values were preliminarily determined through theoretical analysis. At the same time, the digital and discrete element models of the groove-spoon seed displacer were established. Then, single-factor and three-factor five-level quadratic regression orthogonal rotary combination tests were used to simulate the seed displacing performance and explore the structural parameters and working parameters of the seed displacer that significantly affected the test indexes. Subsequently, a second-order regression mathematical model of the significance parameters was established. The parameters of the regression model were optimized, and the optimization results were verified by simulation experiments, bench tests, and field tests to provide references for the optimal design of the cabbage seed displacer structure.

2 Agronomy of Chinese cabbage growing

Chinese cabbage in Northeast China is mainly planted by open-field direct seeding. Usually, it adopts a single-row ridge cropping pattern, as shown in Figure 1. Single row and single hole one seed planting on the ridge, late summer and early autumn sowing (end of July and early August), the spacing of the ridge is 70–75cm, the height of the ridge is 15–20cm, the spacing between plants is 30–40cm, the spacing between the rows is 70–75 cm and the depth of sowing is 2 cm (Yang et al., 2020). The number of seeds sown per hole and the plant spacing provide a basis for the distribution of seed spoons in the seed metering device and the design of the number of circumferential seed spoons.





Schematic diagram of the structure of groove-spoon type Chinese cabbage precision seed discharger. 1. Front shell 2. bearing 3. Seeding groove 4. Seed unloading groove 5. guide ring groove 6. Seed guard 7. Seed layer height adjustment plate 8. Seed box 9. Back shell 10. Seed guide tube 11. Seed spoon.

3 Structure and working principle of the seed metering device

3.1 Structural design of the seed metering device

The seed metering device structure, as shown in Figure 2, is mainly composed of a front shell, seed discharge groove, bearing, seed protection plate, rear shell, seed box, seed spoon, introductory ring groove, and so on; this seeder in the structure of the elimination of the seed guide and seed-clearing components, directly through the seed discharge groove on the seed spoon for the seed, clearing the seed, through the seed introduced area after the seeding unloading, avoiding seed damage caused by shear force or extrusion pressure during the seeding operation, and increase the introductory ring groove and seed unloading groove structure to assist in casting to improve the uniformity of the seed dis-charge.

3.2 Working principle of the seed metering device

When the seed metering device is in operation, the height of the seed layer adjustment plate should be adjusted to an appropriate level. Under gravity, the seeds in the seed box enter the seed-filling area and form a pile. The motor drives the seed discharge groove to rotate. The seed spoon on the seed discharge groove is driven into the seed-filling area. Under the combined action of gravity, centrifugal force, and inter-species force, the seeds fill the holes in the seed spoon. As the seed

discharge groove continues to rotate, it leaves the seed stockpile and enters the seed-clearing area after the seed spoon holes are filled. The excess seeds dragged outside the seed spoon holes slide down to the seed pile under centrifugal force and gravity combined. Then, as the seed spoon rotates with the seed discharge groove over the highest point and enters the seedconduction area, an independent space is formed between the adjacent two seed spoons and the seed guard plate in the seedunloading area. The target seeds in the holes of the discharge spoon are dislodged from the holes by the combined action of gravity and centrifugal force, slide down along the guide seed unloading groove to the back seed unloading groove of the previous seed-excluding spoon, and then reach the seedunloading area with the rotation of the seed discharge groove. Under gravity, the seeds are dislodged from the seed unloading groove into the soil of the seed trench, thus completing one cycle of the seed-metering operation. The principle of the seedmetering device is illustrated in Figure 3.

4 Key component design and parameter analysis

4.1 Determination of seed material properties

The Chinese cabbage groove-spoon-type precision seed metering equipment works similarly to a regular mechanical seed metering system. It uses the fixed size of the seed spoon-type aperture to separate individual Chinese cabbage seeds from the batch. Consequently, the morphology and dimensional

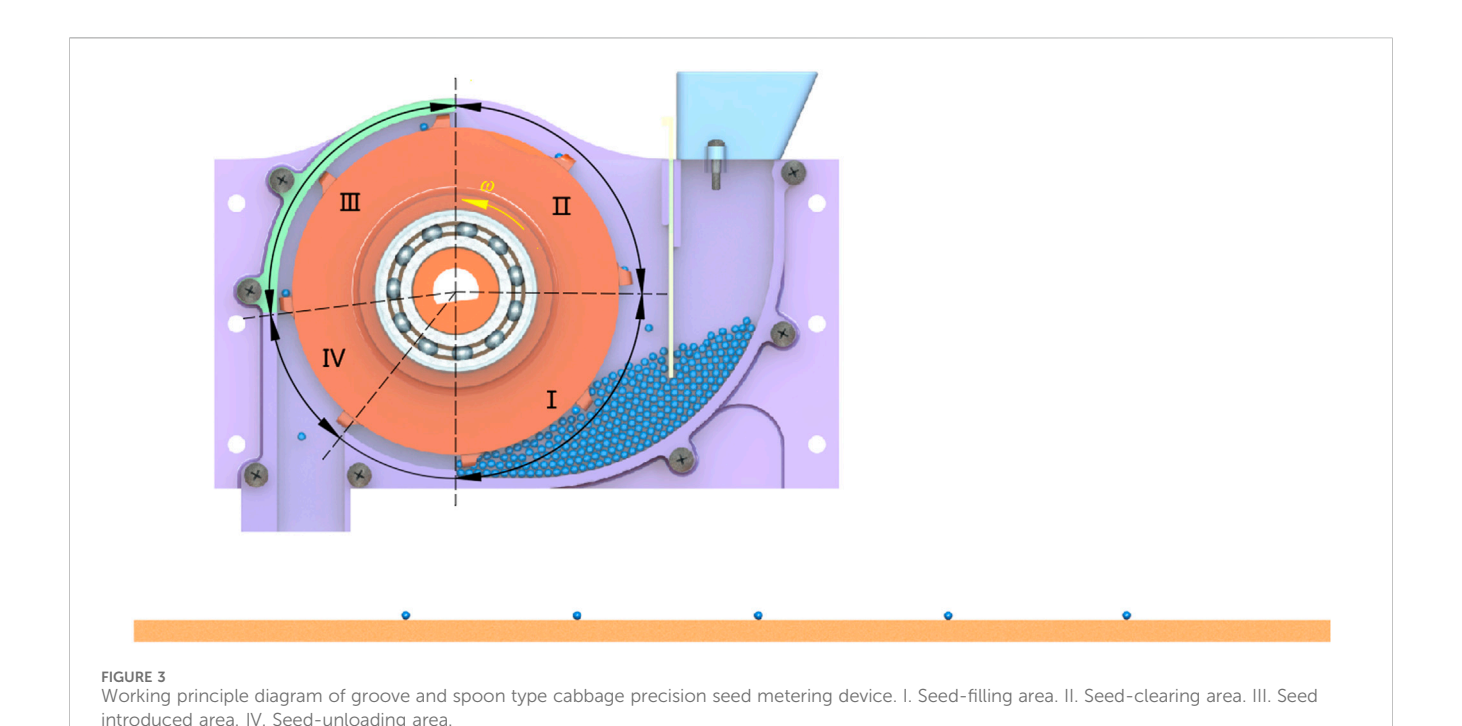


TABLE 1 Triaxial dimensions of Chinese cabbage seeds.

Triaxial dimensions	Maximum value/mm	Minimum value/mm	average value/mm
Length	2.06	1.55	1.79
Width	1.95	1.51	1.73
Thickness	1.87	1.46	1.68

characteristics of Chinese cabbage seeds are a crucial foundation for the design of the seed spoon's shape and volume (Liu et al., 2016). This investigation involved the random selection of 100 Chinese cabbage seeds, possessing a water content of 7.5%, produced by Heilongjiang Jixian Huayi Seed Industry Company. Measurements of the three-dimensional axes (length l, width w, and thickness t) of each Chinese cabbage seed were conducted using digital vernier calipers (range 200 mm, precision 0.01 mm), with the findings presented in Table 1.

Apply Origin 2022 software to statistically analyze the population distribution pattern of sample Chinese cabbage seeds, draw a bar chart, and fit the sample distribution pattern data. As shown in Figure 4, the length, width, and thickness of Chinese cabbage seeds obeyed the normal distribution.

Calculate the equivalent diameter D_e and sphericity S_p of cabbage seeds using Equations 1, 2.

$$D_e = \sqrt[3]{lwt} \tag{1}$$

$$S_P = \frac{D_e}{l} \times 100\% \tag{2}$$

Based on the three-axis mean dimensions of the Chinese cabbage seeds, the equivalent diameter was calculated to be about 1.73 mm, the sphericity was about 96.88%, and the seeds' shape was spheroidal.

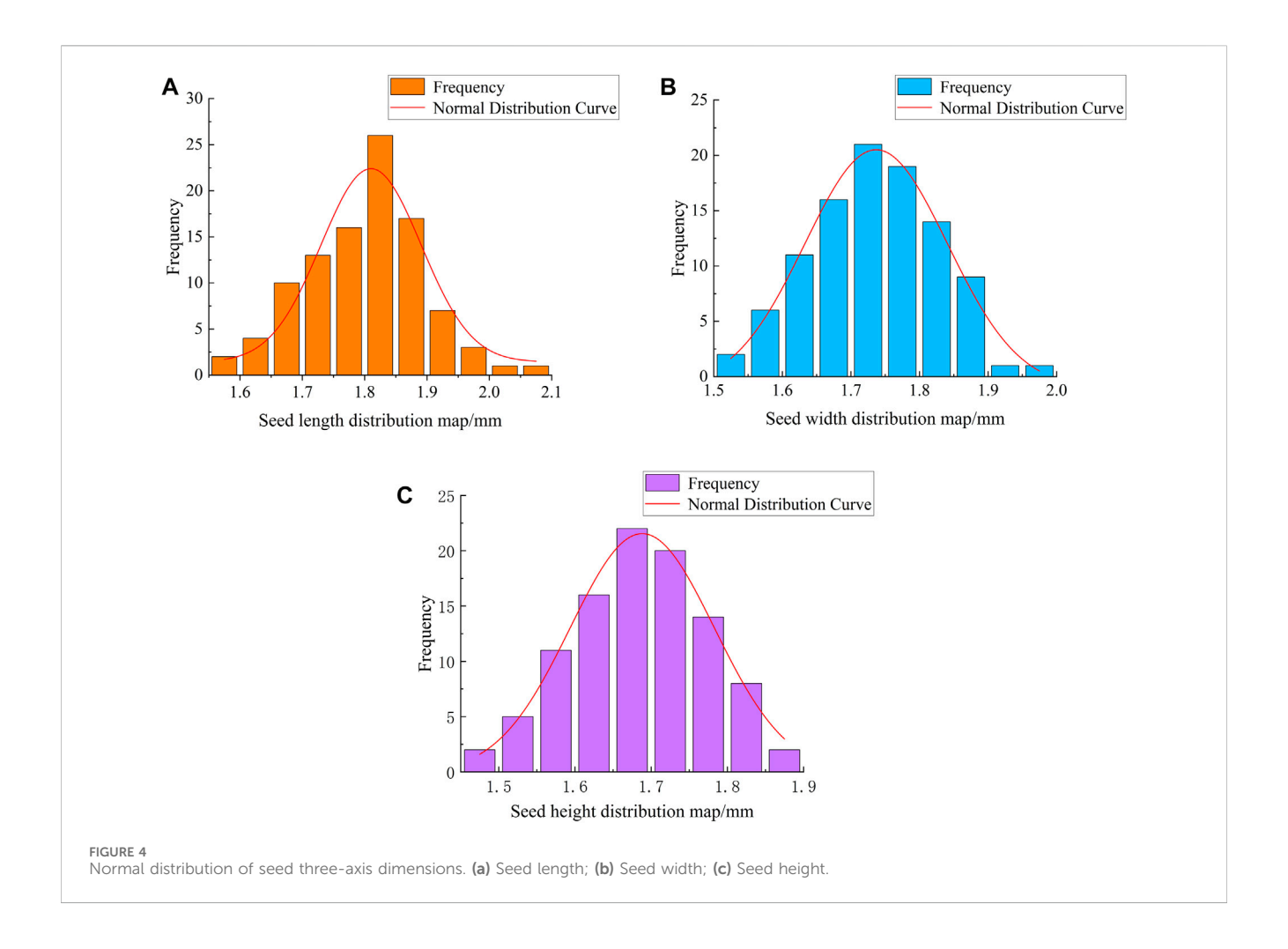
4.2 Design of the structural parameters of the seed spoon

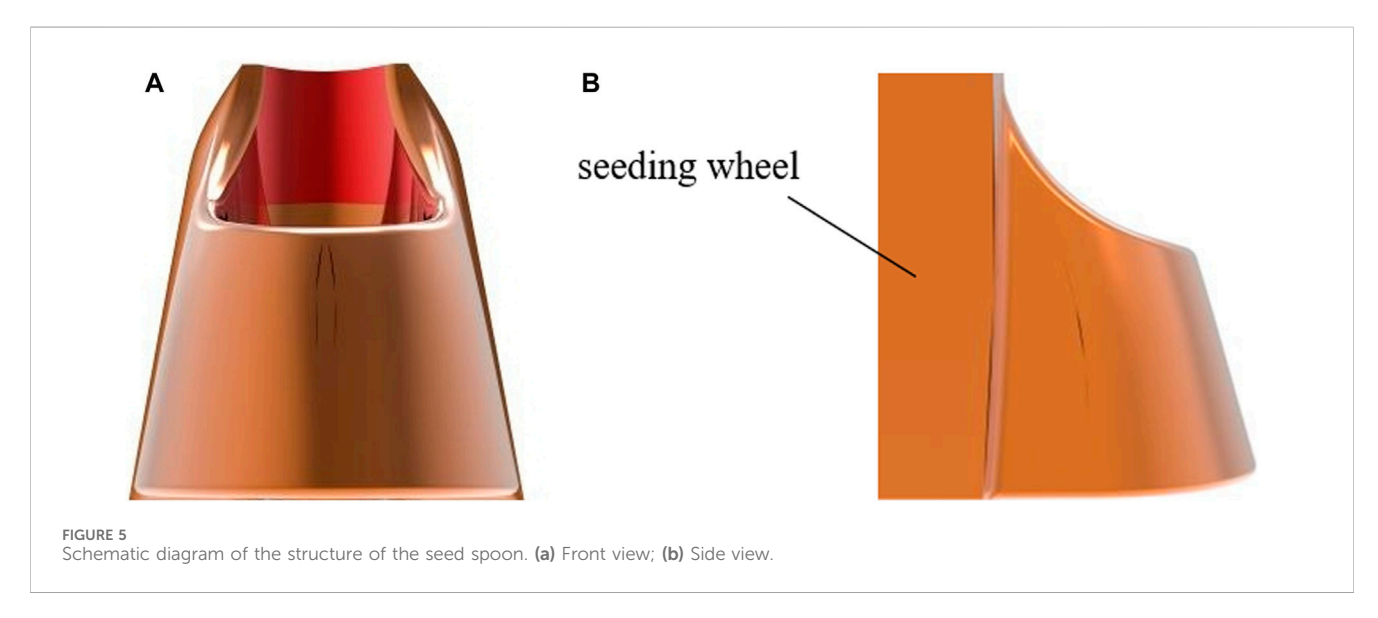
4.2.1 Seed scoop shape design

This paper proposes a tapered seed scoop structure with a "wider bottom and narrower top" to improve the pass rate of single seed sowing of Chinese cabbage seeds. This seed scoop shape prevents the seed scoop from holding excess seed during filling, minimizing the possibility of sowing multiple seeds simultaneously. In addition, this design ensures that the seeding spoon works effectively with the seed protection plate in the seed protection area to create a relatively isolated seed storage area. As shown in Figure 5, the rear of the sowing spoon is integrated into the seed discharge groove, and the entire part is manufactured using 3D printing technology.

4.2.2 Seed spoon-type hole design

The seed scoop serves as the primary conduit for the seed metering device, facilitating the loading and transport of seeds. An effective design of the seed scoop's hole structure characteristics is crucial for achieving consistent seed loading, efficient seed clearing, and preventing seed blockages. The design of the seed spoon-shaped aperture is predicated on the physical characteristics of Chinese cabbage seeds. Based on the principle of sphericity and

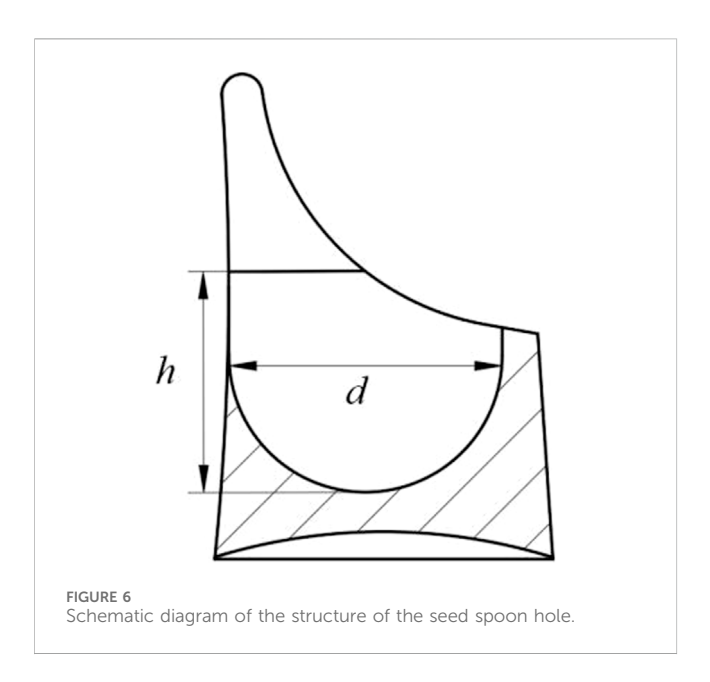




the minimal potential energy of Chinese cabbage seeds, these seeds are round, and all of their different positions in the hole when they are disturbed are the same (Fang et al., 2022). To enhance the efficiency of the seed-filling process, the filling rate becomes increasingly substantial and stable upon entering the hole. To

promote flexibility, the seed spoon hole is built with a "U-hole" structure, as seen in Figure 6.

The design of the seed spoon is intended to accommodate one seed per spoon in accordance with the agronomic requirements for planting Chinese cabbage. To optimize the filling efficiency of the



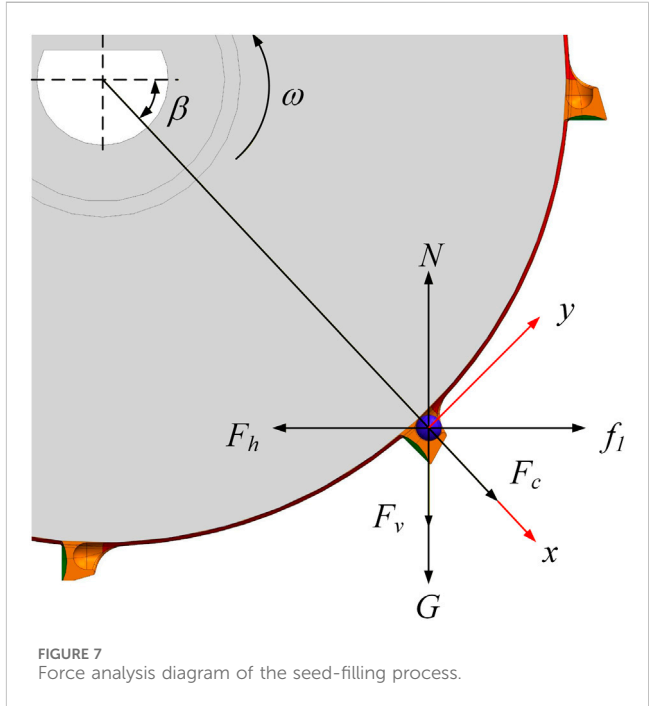
seed hole and prevent seed jamming, the design parameters for the Chinese cabbage seed triaxial size must be considered. The depth of the seed hole, denoted as h, should take into account the seed's center of gravity to prevent easy removal during the clearing process. The diameter of the hole, d, must accommodate at least one particle of the largest seed diameter while preventing the entry of two or more particles of the smallest diameter. The dimensions of the spoon-type hole are critical. Equation 3 is shown below.

$$\begin{cases} d = l_{max} + k, d < 2t_{min} \\ h = l_{max} - j, h \ge w_{min} \end{cases}$$
 (3)

Where: $l_{\rm max}$ is the maximum value of the length of Chinese cabbage seed, mm; $l_{\rm min}$ is the minimum value of the thickness of Chinese cabbage seed, mm; $w_{\rm min}$ is the minimum value of the width of Chinese cabbage seed, mm; k is the gap between the hole wall of the typed hole and the cabbage seed, taking the value of 0–0.84 mm; j is the gap between the upper plane of the typed hole and the Chinese cabbage seed, which takes the value of 0–0.56 mm.

The diameter of the U-hole, d, ranges from 2.06 to 2.90 mm, and the depth, h, ranges from 1.50 to 2.06 mm, as determined by the formula. The structural dimensions of each type of spoon hole are later established by simulation research and empirical testing.

The seamless insertion of Chinese cabbage seeds into the seed spoon aperture is the initial step toward ensuring a consistent seed supply (Dong et al., 2024). The seeds in the filling zone experience the complete disruption effect of the seed-picking groove and the seed-spoon hole. Additionally, some seeds next to the seed spoon hole are deposited into the U-hole due to gravitational force, interseed pressure, and friction. The center of mass of the seed contained within the seed spoon-shaped cavity is designated as the research subject. A second set of coordinates is made based on the normal and tangential directions of the mass system's motion. Any vibrations that the research object feels while it is working are not taken into account. The force analysis of the seeds in the filling area is illustrated in Figure 7, with the corresponding force equation provided below:



$$\begin{cases} F_{h}\cos\beta + N\sin\beta = f_{1}\cos\beta + (F_{v} + G)\sin\beta + F_{c} \\ f_{1}\sin\beta + N\cos\beta = (F_{v} + G)\cos\beta + F_{h}\sin\beta \\ f_{1} = \mu N \\ F_{c} = m\omega^{2}R \\ G = mg \\ \omega = \frac{2\pi n}{60} \end{cases}$$

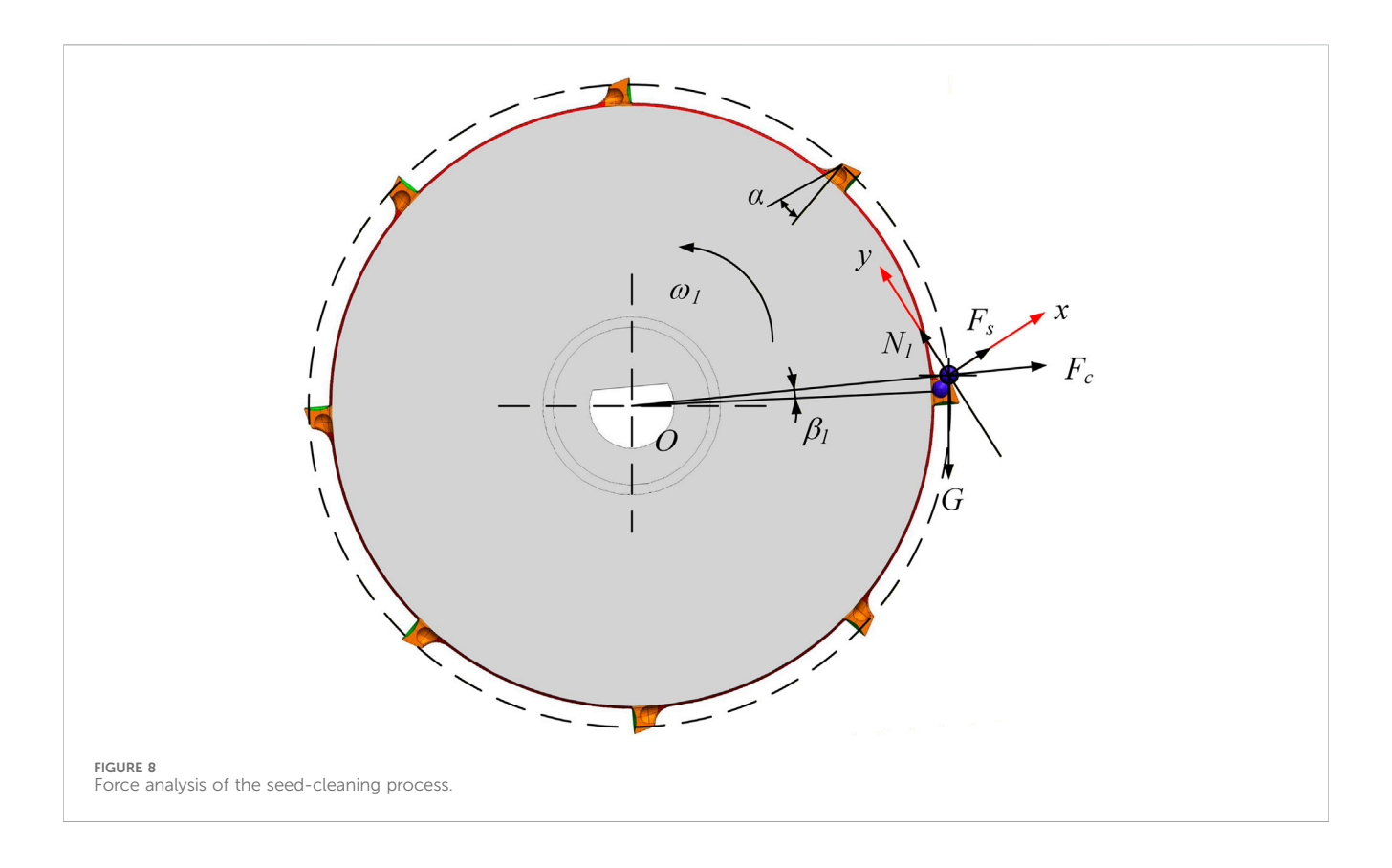
$$(4)$$

Where: N is the support force of the spoon hole on the Chinese cabbage seed, N; β is the initial filling angle, $^{\circ}$; F_h is the horizontal pressure of the seed population on the seed centre of mass in the filling area, N; F_v is the vertical pressure of the seed population on the seed centre of mass in the filling area, N; G is the gravitational force of the seed, N; F_c is the inertial centrifugal force of the seed, N; f_1 is the friction between the seed and the inner wall of the hole, N; μ is the friction coefficient of the surface of the seed and the hole, taken as 0.46; m is the seed mass in the hole, kg; ω is the seeding groove angular velocity, rad/s; g is the acceleration of gravity, 9.81 m/s²; n is the seed extraction groove's rotational speed, r/min; R is the radius of the seeding groove, mm.

From Equation 4

$$\beta = \arcsin \frac{F_c (N - F_v - G)}{(F_h - f_1)^2 + (N - F_v - G)^2}$$
 (5)

What Equation 5 shows is that the population's horizontal pressure F_h on seeds in the filling region is affected by the initial filling angle β , the friction f_1 between the seed and the hole's inner wall, the seed extraction groove's rotational speed n, and other factors. As the structural properties of the hole type and processing materials are known, the initial filling angle β gets smaller as the seeding groove speed n goes up. The appropriate lowering of seeding groove speed can prolong the filling duration, hence enhancing the stability of the filling process.



4.2.3 The top inclination angle of the seed spoon

A study of the seed-clearing process focuses on the external hole connected to the drag that holds the seeds and how the forced drag interacts with the seed layer. The study centers on the external hole, treating it as the primary subject due to the bulk accumulation of seeds. Consequently, the row of seed spoon-type holes with excess seeds is analyzed collectively to ascertain the critical state of seed clearing. The force is seen in Figure 8.

The seeding groove rotates around the seed discharge axis, and the dragged seeds make a parabolic falling motion along the seed spoon relative to the seeding groove. The force analysis of the dragged seed group can be obtained as follows:

$$\begin{cases} G\sin(\beta_1 + \alpha) - F_s - F_c\cos\beta_1 = m\alpha_t \\ F_c\cos\beta_1 + G(\cos\beta_1 + \alpha) = N_1 + m\alpha_I \\ F_S = \mu_2 N_1 \sin\beta_1 \end{cases}$$
 (6)

Where: α is the angle between the tangent line at the top of the seed spoon and the top of the seed spoon; N_I is the support force of the seeds in the type hole on the dragged seed group, N; F_s is the friction force of the seeds in the type hole on the dragged seed group, N; F_c is the Coriolis inertial force, N; φ is the natural angle of repose of the cabbage seed, (°); a_t is the acceleration of the seeds falling along the seed picking spoon, m/s 2; a_I is the seed Coriolis acceleration, m/ s²:; μ_2 is the Coefficient of Friction Between Seeds, 0.491; β_1 is the seed group clearance angle, (°).

From Equation 6, the angle of seed clearing is

$$\beta_1 = \arctan \frac{ma_t + \mu_2 F_N + F_c \cos \alpha}{F_N + ma_I - F_c \sin \alpha} - \alpha \tag{7}$$

Equation 7 shows that the seed group clearance angle β_1 is connected to factors such as the seed spoon's top inclination angle α , the spoon groove's angular velocity ω , and the cabbage seeds' natural resting angle ϕ . When the rotational speed aligns with the support force, the clearance angle $\beta 1$ exhibits a negative correlation with the tip inclination angle of the seed spoon. When the seed spoon is positioned at a specific tip inclination angle, it facilitates the timely descent of extra seeds from the outer side of the drilled hole, preventing reseeding. Alterations in the upper inclination angle of the seed spoon will influence the efficacy of seed clearing. If the maximum inclination angle of the seed spoon is excessive, the intended seeds within the seed spoon hole will begin to fall downward prior to reaching the seed introduction area, leading to seed spillage. If the seed spoon's upper inclination angle is insufficient, surplus seeds will remain, leading to re-sowing. The inherent rest angle ϕ of Chinese cabbage seeds is 26.08°, in conjunction with the structural parameters of the seed spoon. The optimal inclination angle of the seed spoon is designed to vary from 0° to 26°.

4.2.4 Number of seed spoons

The main structure of the seed metering device is the seed spoon distribution. If the planter's forward speed and plant spacing stay the same, the U-hole groove spoon seed metering device's filling frequency depends on the number of seed spoons and the seeding groove's linear speed. An increased quantity of seed spoons correlates with a diminished groove speed (Du et al., 2019; Li H. et al., 2024). The extended duration a single seed spoon remains in the seed-filling zone enhances the seed-filling

rate of the seeder and augments seeding stability (Ding et al., 2024; Zhang et al., 2020). As a result, the number of seeding spoons should be increased as needed, as long as the shape and size of the seeding groove allow two adjacent spoons to work without any problems. The quantity of seed spoons must be adequate:

$$\begin{cases}
Z = \frac{\pi D_d V_m}{SV_d (1-c)} \\
V_d = \frac{\pi D_d n}{60}
\end{cases}$$
(8)

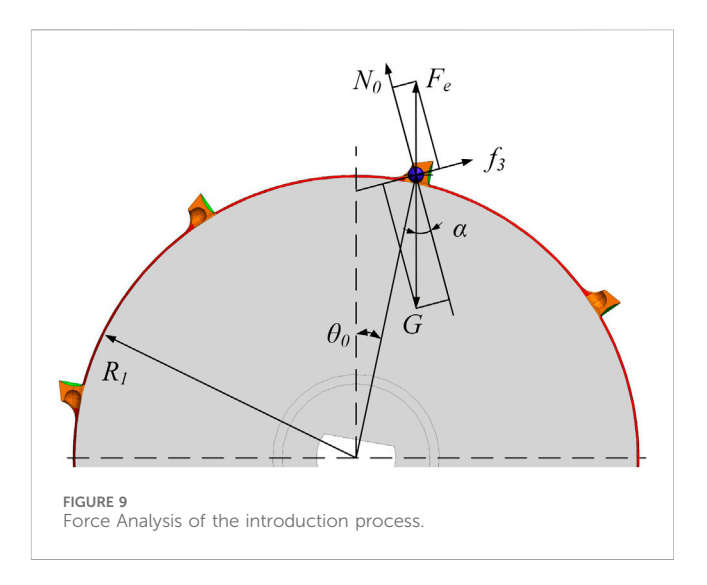
Where: Z is the number of seed spoons arranged on the circumference of the seeding groove, one; D_d is the diameter of the circle corresponding to the centre of the inner hole of the seed spoon, mm; V_m is the forward speed of the hand-push planter, m/s; S is the sowing distance between Chinese cabbage seeds, m; V_d is the linear velocity at the centre of the inner hole of the seed spoon, m/s; c is the slip coefficient of the ground groove; n is the operating speed of the seeding groove, r/min; From Equation 8

$$Z = \frac{60V_m}{nS(1-c)} \tag{9}$$

This document discusses the installation of a seed metering device on a hand-push planter for testing, with the planter's operational forward speed typically ranging from 0.4 to 1.2 m/s, specifically set at $V_m = 0.8$ m/s. Based on the agronomic specifications for cabbage seeds, the typical planting distance ranges from 0.30 to 0.40 m, with a selection of S = 0.30 m. The seed rower utilizes an electric drive controlled by an electric system for power, with a ground groove slip coefficient of c = 0. The operating speed of the row seeding groove is primarily utilized to gather the real-time forward speed of the planter, enabling the adjustment of the seeding groove's rotation speed via a GPS receiver. Based on the operational speed of the seeding machine and the requirements for sowing spacing, an optimal seeding groove speed of 20 r/min is selected. Consequently, it is calculated that eight seed spoons can be installed around the circumference of the seeding groove, with two adjacent seed spoons corresponding to a central angle of 45° from Equation 9.

4.3 Seeding groove diameter

The diameter of the seeding groove is a crucial component influencing the seed discharge efficiency of the seed metering apparatus. The filling frequency of the U-hole groove spoon seeder is contingent upon the number of seeding spoons and the linear velocity of the seeding groove, given a certain forward speed of the planter and plant spacing. As the diameter of the seed groove increases, the speed will correspondingly drop, resulting in an extended filling time. This enhancement is beneficial for boosting the filling coefficient; nevertheless, it will also lead to an increase in the overall dimensions of the seed metering device. A smaller diameter will result in an increased rotational speed and a corresponding reduction in filling time, which may lead to leakage of seed filling or insufficient charging. This situation is detrimental to seeding uniformity and adversely affects the quality of seeding discharge (Li Y. et al., 2024). To examine the impact of seeding groove diameter on the filling time of the seed spoon,



equations relating filling time t to the diameter of the seed groove were formulated from Equation 10:

$$\begin{cases} t = l_j / v_d \\ l_j = \beta_c (R+r) \\ v_d = 2\pi n (R+r) \end{cases}$$
 (10)

Where: l_j is the arc length of the seeding area, mm; β_c is the angle of the seeding area, rad; R is the radius of the seeding groove, mm; r is the radius of the seed spoon, mm; n is the operating speed of the seeding groove, r/min from Equation 11.

$$t = \frac{\beta_c}{2\pi n} \tag{11}$$

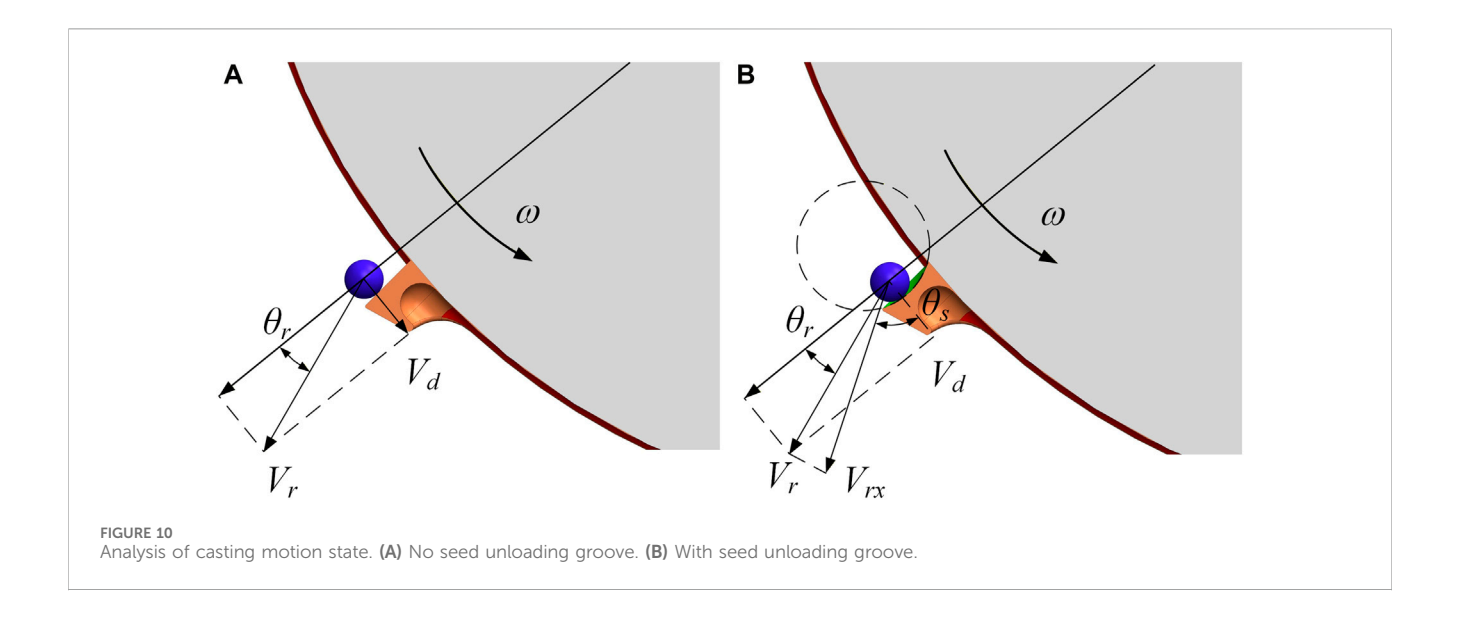
Equation 6 indicates that the seed filling duration of the seed spoon is only dependent on the angle of the seed filling area and the velocity of the seeding groove, with no correlation to the diameter of the seeding groove. Regardless, changing the diameter of the seeding groove will cause changes in the number of seed spoons, the seeding groove's linear speed, the seeding groove itself, and the overall structure dimensions of the seed metering apparatus. According to the "Agricultural Machinery Design Manual" (2007), the structural design of the seed dispenser in the hand-push planter requires miniaturization. This research meticulously examines the seeding groove diameter *D* of 80 mm.

4.4 Guide ring groove design

The seed guide mechanism facilitates the movement of the cabbage seed along the seed introduction ring groove towards the seed unloading groove. During this process, the seeds are affected by their own weight, centrifugal force, friction, and support force. Figure 9 shows a force analysis of the seed guidance process.

Assuming that the cabbage seed is in force equilibrium at this point, a hydrostatic analysis of it yields from Equation 12:

$$\begin{cases} mg \sin \alpha = f_3 + F_c \cos(\alpha + \theta_0) \\ N_0 + F_c \sin(\alpha + \theta_0) = mg \cos \alpha \end{cases}$$
 (12)



Equation 13 simplifies to $\tan \alpha \ge \frac{\omega^2 R \cos(\alpha + \theta_0)}{g + \omega^2 R \sin \theta_0}$, since θ_0 is close to zero and $0 < \alpha < 30^\circ$, simplifies to:

$$R_1 \le \frac{\tan \alpha g}{\omega^2} \tag{13}$$

From Equation 14, we can see that the radius of the guiding ring groove depends on how fast the seed metering device turns and the angle between the vertical orientations. The angular velocity ω of the seed-measuring device groove is determined from Equation (4) to be 2.09 rad/s. When $\alpha = 16^{\circ}$, inserting this value into Equation (14) yields a guide ring groove radius $R_1 \le 67.40$ mm. The radius of the seeding groove, R, is 40 mm; hence, the radius of the guide ring groove, R_I , must be smaller than 40 mm. Given that the average diameter of Chinese cabbage seeds is 1.73 mm, it is essential to ensure that the radius of the guide seed unloading groove is appropriately sized. If the radius is excessively large, the seeds may collide with the surface of the seeding groove in the seed unloading area, resulting in damage. If the radius is too small, on the other hand, the seeds could get stuck at the corner between the guide seed unloading groove and the seed spoon seeding groove that comes before it, which would stop the seeding process. For thorough evaluation, the radius of the seed introduction ring groove R_1 is established at 39.7 mm, with the width of the ring groove matching the diameter of the U-hole.

4.5 Force analysis of the seed-unloading

Uniform and stable seed-unloading in the seed-unloading area is a key factor affect-ing the performance of the seed metering device (Sun et al., 2024). The rapid rotation of the seeding groove allows for an optimal seed-unloading speed vector, significantly minimiz-ing collisions between the Chinese cabbage seeds and the seed metering apparatus. This keeps the seeds moving smoothly inside the device and improves the even distribution of seeds. This paper looks at how seeds move when they are about to come out of a spoon-shaped hole. It does this by comparing situations with and without a seed unload-ing groove.

The motion of the seeds was analyzed when they were about to leave the no seed unloading groove (Figure 10a), at which time the

Chinese cabbage seed-unloading speed satisfied the following relationship:

$$\begin{cases} V_d = \omega R_2 \\ V_r = \frac{V}{\sin \theta_r} \end{cases} \tag{14}$$

Where: R_2 is the distribution radius of the seed spoon hole, mm; V_d is the linear velocity at the centre of the hole, m/s; V_r is the seed-unloading speed when the seed leaves the no-seed unloading groove, m/s; V_r is the linear speed of forming Groove, m/s; V_r is the seed-unloading angle, °.

Analyze the motion state when the seed is about to leave with the seed unloading groove (arc-shaped hole) (Figure 10b); at this time, the seeding speed of the Chinese cabbage seed satisfies the following relationship:

$$\begin{cases} V_t = \frac{V_{\omega}}{\cos \theta_s} \\ V_{tx} = V_t \sin(\theta_r + \theta_s) \end{cases}$$
 (15)

According to Equation 15, the seed-unloading velocity V_r when the seed leaves the no seed unloading groove can be converted into:

$$V_r = \frac{V_d \left(\sin^2 \theta_r + \cos^2 \theta_r\right)}{\sin \theta_r} = V_d \sin \theta_r + \frac{V_d \cos \theta_r}{\tan \theta_r}$$
 (16)

According to Equation 16, the casting velocity V_{tx} at which the seed leaves a with seed unloading groove (arc-shaped hole) can be converted into:

$$V_{tx} = V_d \sin \theta_r + V_d \cos \theta_r \tan \theta_s \tag{17}$$

According to Equations 17, 18, the seed velocity V_r of seeds exiting the no seed unloading groove exceeds the seed velocity V_{tx} of seeds departing from the with seed unloading groove. The motion of seeds exiting the no-seed un-loading groove can be approximated as horizontal parabolic motion with an initial velocity of V_r . Consequently, the likelihood of seeds colliding with the seed discharge tube and altering their direction upon exiting the no-seed unloading groove is considerably high. Simultaneously, the incidence of seed damage escalates while the seed flow direction remains consistent

TABLE 2 Parameters of materials required for seeding simulation.

Project	Attributes	Value		
Chinese cabbage seeds	Poisson's ratio	0.356		
	Shear modulus/Pa	5.24×10^{7}		
	Density/kg·m ⁻³	1,105		
PLA plastic	Poisson's ratio	0.43		
	Shear modulus/Pa	1.3 × 10 ⁹		
	Density/kg·m ⁻³	1,240		
PMMA	Poisson's ratio	0.33		
	Shear modulus/Pa	8.2 × 10 ⁷		
	Density/kg·m ⁻³	1,218.9		
Chinese cabbage seeds -Chinese cabbage Seeds	Restitution coefficient	0.209		
	Static friction coefficient	0.407		
	Rolling friction coefficient	0.173		
Chinese cabbage seeds -PLA plastic	Restitution coefficient	0.566		
	Static friction coefficient	0.455		
	Rolling friction coefficient	0.150		
Chinese cabbage seeds -PMMA	Restitution coefficient	0.607		
	Static friction coefficient	0.396		
	Rolling friction coefficient	0.141		

and uniform. As the seed exits the arc-shaped aperture of the seed slot, it glides smoothly over the surface of the slot, maintaining a consistent flow direction and exhibiting excellent discharge uniformity.

The dimensions of the arc-shaped slot hole influence seed unloading; if excessively large, seeds may remain stationary within the hole. Beyond the seed unloading zone, seeds will descend, heightening the leakage rate. Conversely, if the hole is too small, seeds may prematurely fall, resulting in collisions within the seed guide tube, thereby affecting the uniformity of seed discharge. To ensure the seed transitions smoothly from the guide slide into the slot hole and subsequently descends from the slot hole, the diameter of the seed slot, dc, must match the dimensions of the rear of the seed spoon. Additionally, the depth of the seed unloading groove, h_{c} should be less than the seed's center of gravity. The minimum thickness of the seed, time, is established at 1.46 mm; therefore, the design for the seed slot depth, h_{c} is set between 0.1 mm and 0.70 mm, which will be further examined through simulation.

5 Simulation test of seed dispenser performance

5.1 Simulation modeling and simulation parameter determination

5.1.1 Simulation parameter setting

Because Chinese cabbage seeds have a smooth, non-sticky surface, the Hertz-Mindlin (no-slip) model was chosen as the

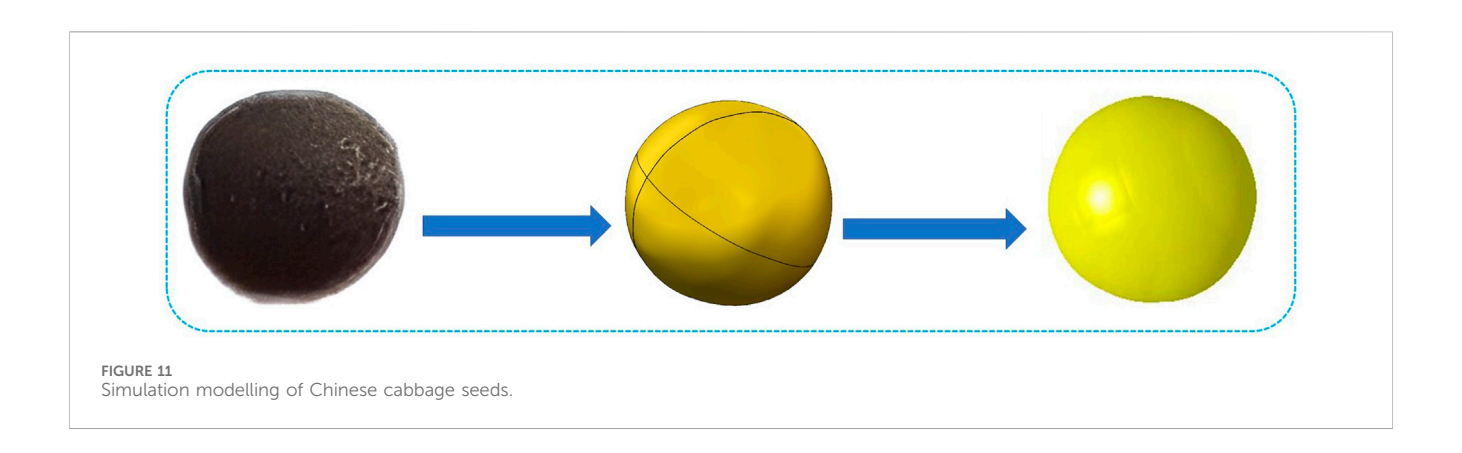
simulation contact model for how seeds interact with each other and with contact materials (Wang et al., 2022). In the operation of the seed metering device, all components in touch with the seeds, save for the front shell made of PMMA (Polymethyl methacrylate), are fabricated using 3D rapid prototyping technology with PLA plastic as the material. The results of this study, which included both experiments and a review of the literature, show the basic physical properties and interfacial mechanical properties of cabbage seeds and seed dispenser materials (PMMA and PLA plastics) (Dun et al., 2024; 2023; Zhang et al., 2024) (Table 2).

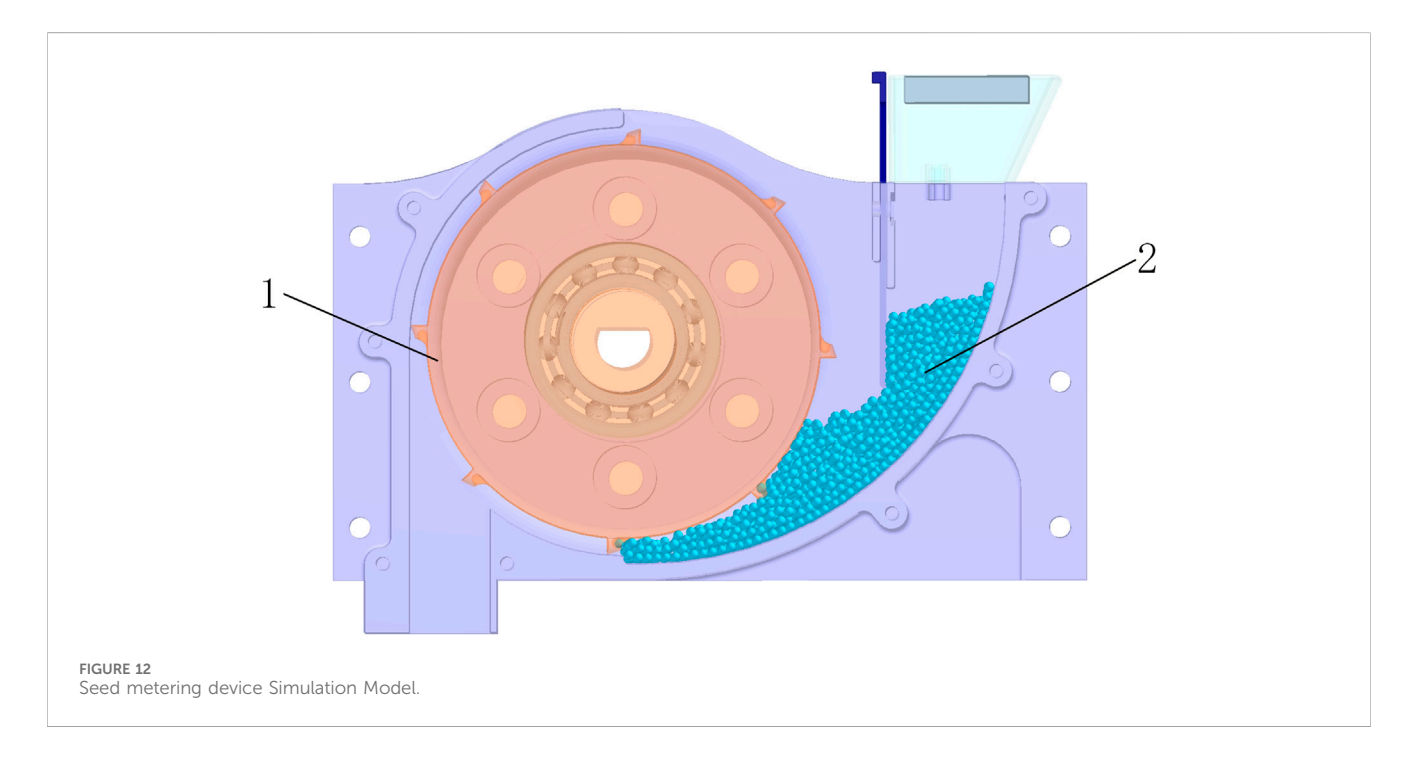
5.1.2 Simulation modelling of Chinese cabbage seeds

To make the seed discrete element model consistent with the actual seed model, ac-cording to the average value and shape of the three-axis size determination of the cabbage seed in the previous period, the SolidWorks 2023 software was used to draw its three-dimensional model and save it in STL format for importing into EDEM 2020 soft-ware. The seed simulation model was obtained by spherical filling, as shown in Figure 11.

5.1.3 Simulation modelling of seed dispenser

Based on the previous structural design and kinematic analysis of the seed metering device, it was modeled in a 1:1 scale using SOLIDWORKS 2023 software. To make the simulation run faster without affecting the results, the model was made simpler and exported in STL format to import it into the EDEM 2020 software. Table 2 shows how to set up each variable





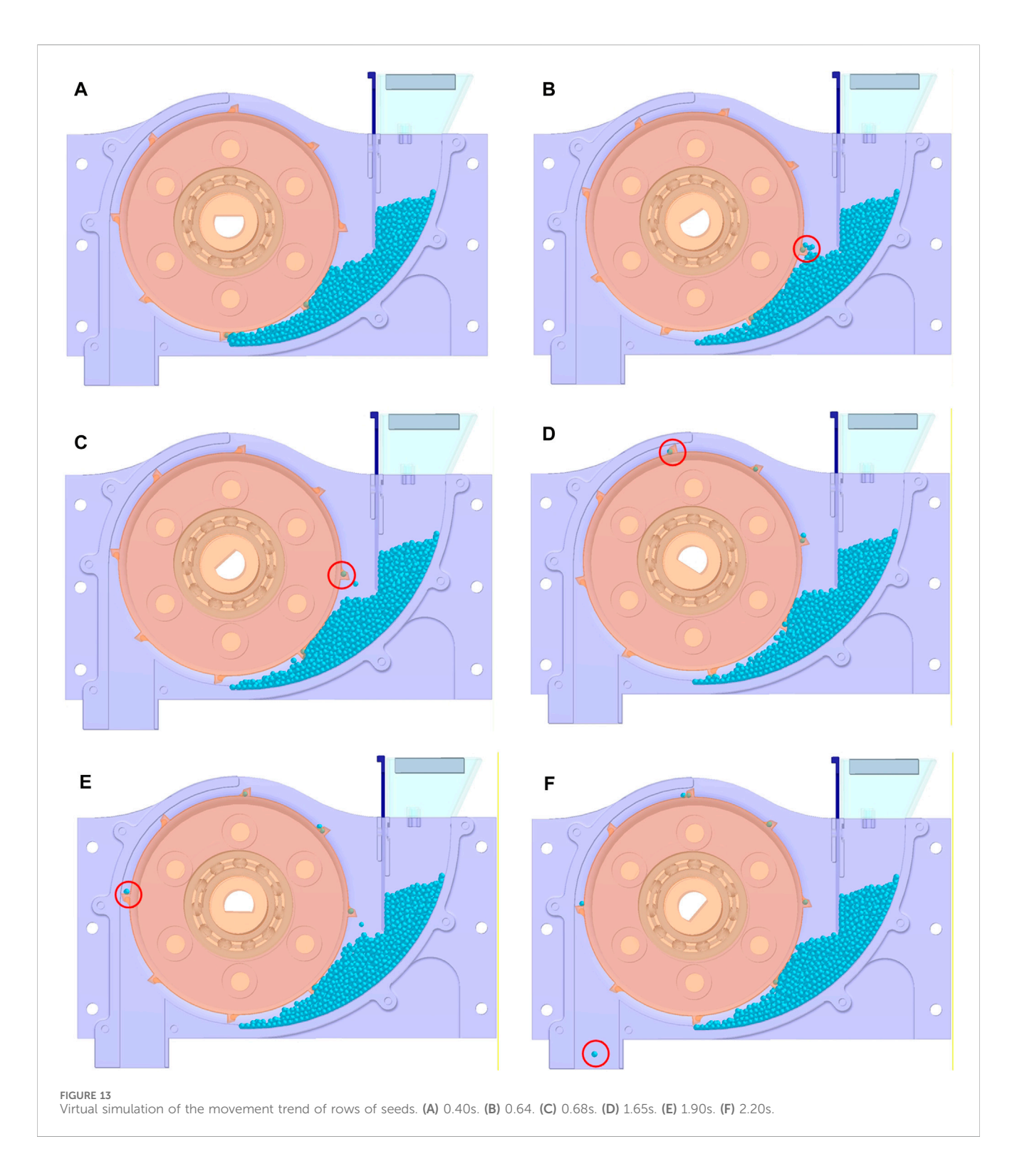
component. The particle factory was constructed above the seed box to dynamically produce Chinese cabbage particles, totaling 1,200 particles at a production rate of 3,000 per second. The seed size followed a normal distribution, with a standard deviation of 0.1, and the particle size limits ranged from a minimum of 0.85 times the mean to a maximum of 1.17 times the mean. A linear rotary motion is introduced to the seed picker groove, initiating movement at 0.4 s the time step is 3.44×10^{-6} s, and the data saving interval recording time is 0.01s. Figure 12 illustrates the simulation model of the seed metering apparatus.

5.1.4 Simulation modelling of seed dispenser

Based on the pertinent parameter configurations, simulate the real operational process of seed discharge, conduct a virtual simulation analysis of the various operational linkages of the seed metering device, and examine the primary causes of seed multiplicity and leakage.

For better viewing, the front shell's transparency was set to 0.1, as shown in Figure 13. The movement and path of each seed during the seed loading, seed clearing, seed priming, and seed unloading

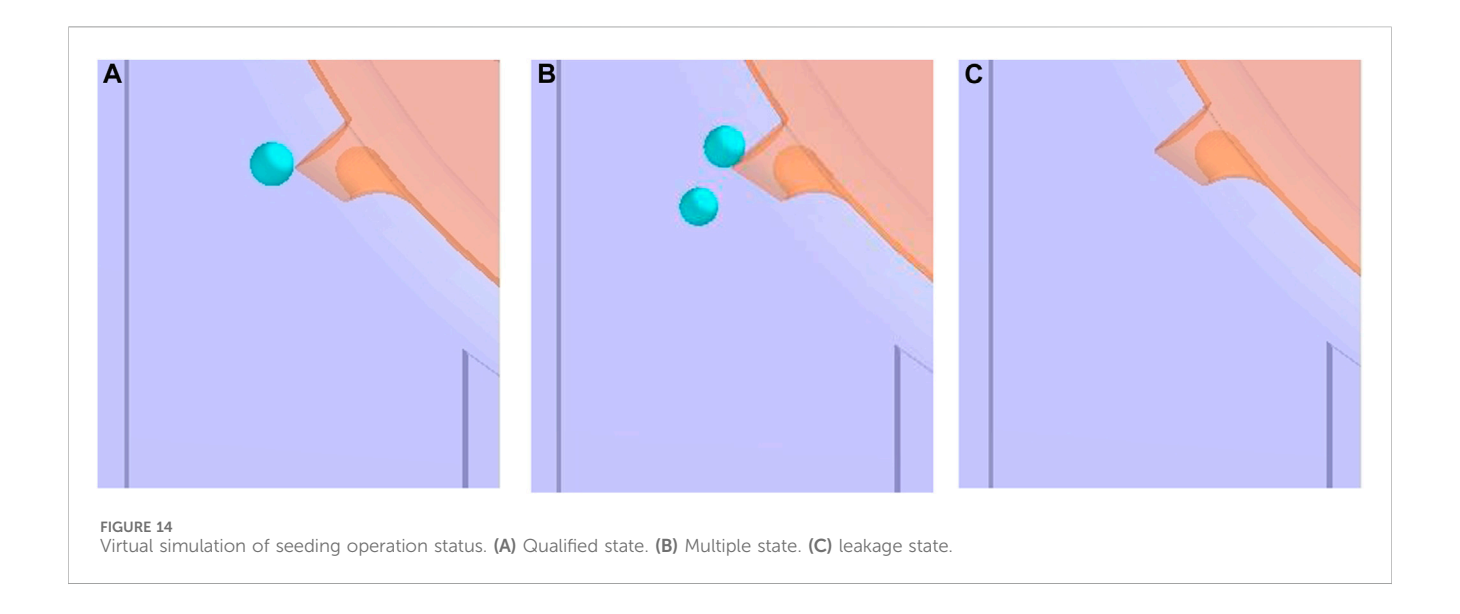
processes in the seed dispenser were studied at each time. Between 0 and 0.4 s, the particle factory made 1,200 different models of Chinese cabbage seeds. These gathered in the seed-filling area because of gravity and the seeds' own weight. After 0.4 s, initiate the uniform circular motion of the seeding groove at a speed of 20 r/ min while simultaneously activating the seed spoon movement. As the seed spoon transitions to the seed-filling zone, the seed descends due to its own gravitational force and the combined extrusion pressure from the species, resulting in the completeness of the seed-filling process. What is the typical function of the seedfilling process in the seed spoon to finalize the seed filling? When the seeding groove moves from the seed-filling zone to the seedclearing zone at 0.75 s, the extra seeds in the seed spoon fall back to the seed pile because of gravity. This completes the seed-clearing process. After 1.34-1.50 s, when the seed spoon reaches the top of the seed-taking groove, gravity and centrifugal force push the target seeds out of the hole. They then fall down the seed-introducing chute and hit the back of the previous seed spoon, ending the seed introduction process. The seeds finally get to the seed-unloading area when the seeding groove turns. They fall through the seed

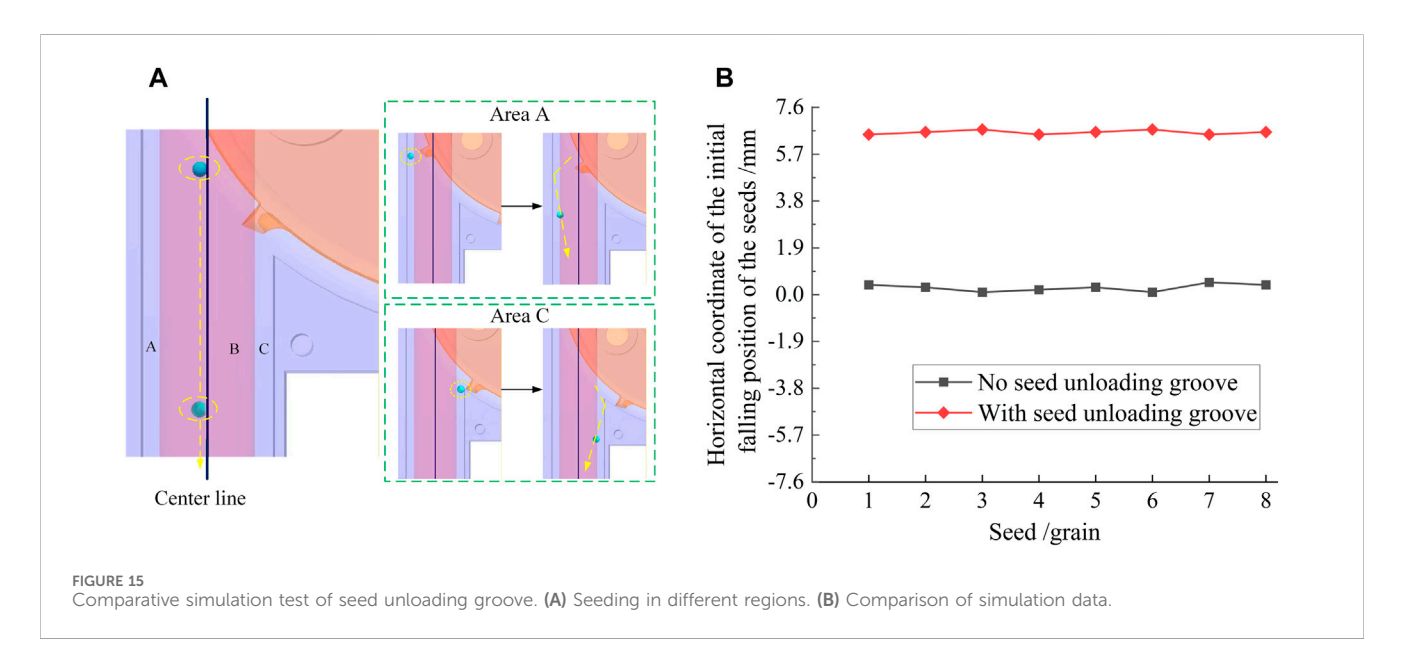


guiding tube from the seed unloading groove into the soil of the seed trench, carried by gravity. The simulation process matches the theoretical analysis of the seed metering device's operational state. This shows that it is possible and valid to do experimental research on the numerical simulation of seed discharge performance.

Figure 14 shows that the three seeding states—single sowing, reseeding, and missed seeding—mostly determine how well the seed

dispenser works during the simulation process. Single seeding is a sowing-qualified condition characterized by the presence of only one seed in the seed-unloading region designated for seeding. The repeat seeding condition occurs when two or more seeds are present in the seed-unloading area for seeding. The primary cause of reseeding is the significant size disparity among Chinese cabbage seeds, which results in multiple smaller seeds occupying the seed spoon-type hole. Because of gravity, the extra seed balances and



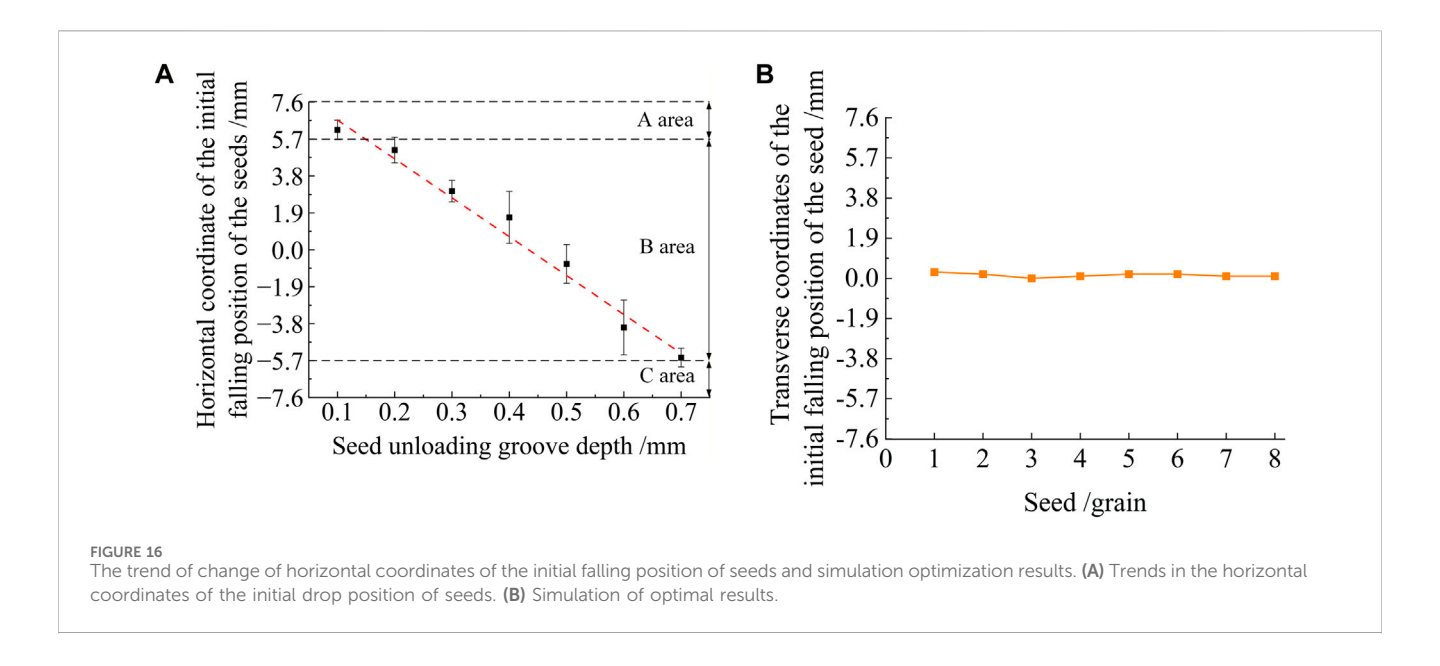


stabilizes the forces between the seeds and the force that holds up the seed spoon row. The leakage state refers to the movement of the seed discharge spoon towards the seed-unloading area without any seeds being released from the discharge opening. The main reason there is no grain is that the seeds in the clearing area can't fight against the pull of gravity. The friction from other seeds and the centrifugal force from the spoon-shaped holes keep the seeds from breaking away from the rest of the seeds.

5.2 Comparative simulation test of seed unloading groove

Theoretical analysis in Section 3.4 shows that seed discharging is more even when there is a seed unloading groove than when there is none. To make sure the theoretical study was correct, a simulation test was done to see what would happen if the seed unloading groove

was added or taken away, while all other factors stayed the exact (Figure 15). Upon arrival at the seed-unloading area from the rear of the seed spoon, the seed descends and is expelled through the seed guide tube. If the seed's initial drop position in Figure 15a is within the row of seeds in Region B, the seed drop process will not contact the wall and will descend smoothly. Conversely, if the seed is positioned in the row of seeds in the drop region, it will contact the left side of the wall during its descent; similarly, if the seed is located in the row of seeds in the drop region, it will contact the right side of the wall. These two "wall" phenomena will alter the seed's trajectory, resulting in uneven seed spacing and adversely affecting the quality of the seed row. As a result, the positional data of the seed during its initial descent is collected during the simulation test. The centerline of the seed guide tube is used as the baseline. On this baseline, the left side is the positive direction, and the transverse coordinates of the seed's initial falling position are found by computing the distance from where the seed is falling now to the



baseline. The horizontal coordinates of the seeds' starting descent location were used as the evaluation metric to assess the seed discharge efficacy of the seed metering mechanism, both with and without the seed unloading groove. For each model, the horizontal coordinates of where the seeds first fell were constantly recorded for one full rotation, which is eight seeds. Figure 16b shows the results.

As can be seen from Figure 15b, when there is no seed with a seed unloading groove, the horizontal coordinate of the initial falling position of the seeds is in the region of a. This means that they will hit the left wall of the seed discharge tube, which will change their path as they fall. On the other hand, if there is a seed discharge slot ($h_c = 0.35$ mm), the initial falling position's horizontal coordinate moves to region b. This lets the seeds fall smoothly. Consequently, seed discharge is more consistent with the presence of a seed slot, and the outcomes of the simulation comparison test align with the theoretical analysis.

As indicated in Section 4.5, the depth of the slot hole ranges from 0.1 to 0.7 mm. To learn more about how the depth of the seed feeding slot affects the even distribution of seeds, the depth of the slot hole and other depths are divided into seven groups. Then, simulation tests will be run while all other factors stay the same. The transverse coordinates of the seeds' starting descent point serve as the evaluation metrics. At each level of the simulated data, the transverse coordinates of where the seeds first fell are recorded as a full circle of eight seeds. Their mean values and standard deviations have been calculated. We found the mean value and standard deviation and then used linear regression to look at the transverse coordinates of where the first seed fell at different depths of the seed unloading groove, as shown in Figure 16a.

The corrected coefficient of determination for this regression model is 0.98, above 0.75. Consequently, the model is well-suited, and it can be demonstrated that the depth of the seed unloading groove significantly influences the efficacy of seed discharge. The regression equation for the fitted linear model is:

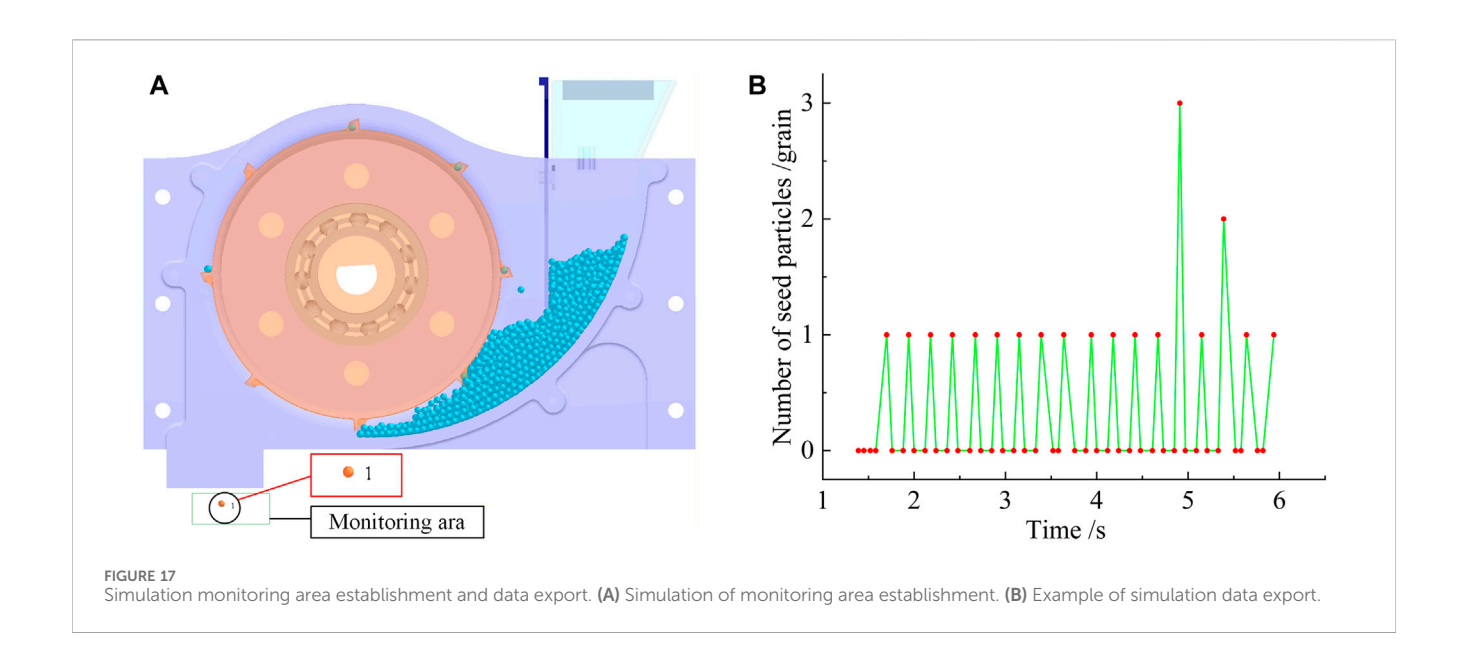
$$y_c = -20.02h_c + 8.68 \tag{18}$$

When the seed's initial drop point is at the center of the seed guide tube, with a horizontal coordinate of 0, the seed does not readily "contact the wall" and can descend gently through the sand. With this information, the equation can be solved to find the seed's initial position as it falls, where y_c is 0, and h_c is the depth of the seed unloading groove. The results of the seeding simulation verification test are illustrated in Figure 16b. Thus, this paper will focus on the design of the seed unloading groove at a depth of 0.43 mm. The corrected coefficient of determination for this regression model is 0.98, above 0.75. Consequently, the model is well-suited, and it can be demonstrated that the depth of the seed un-loading groove significantly influences the efficacy of seed discharge. The regression equation for the fitted linear model is.

5.3 Single factor simulation test

5.3.1 Test factors and test indicators

The structural features of the seed spoon are critical factors influencing the operational efficacy of the seed metering device. Appropriate structural characteristics can significantly enhance the success rate of individual seed filling. EDEM software was used to run a one-factor simulation test to see how different structural parameters affected the seed metering device's ability to work. Based on the previous theoretical study, the test variables were the U-hole diameter, the U-hole depth, and the angle of tilt of the seed scoop's apex. The following range of values was set for each variable: U-hole diameter ranges from 2.06 to 2.90 mm, U-hole depth ranges from 1.50 to 2.06 mm, and the inclination angle of the top of the seed spoon varies from 0° to 26°. The qualified rate Y_1 , the multiple rate Y_2 , and the leakage rate Y_3 were used as performance indicators for the seed metering device, and they were calculated using the formula in line with GB/T 6973-2005 Test Methods for Single Grain (Precision) Seeders and the agronomic specifications for planting Chinese cabbage seeds which was calculated by the Equation 19:



$$Y_1 = \frac{M_1}{M} \times 100\%$$

 $Y_2 = \frac{M_2}{M} \times 100\%$ (19)
 $Y_3 = \frac{M_3}{M} \times 100\%$

Where: M is the theoretical number of seed-unloading ports; M_1 is the number of times 1 seed is discharged from the seed-unloading port; M_2 is the number of times 2 or more seeds are discharged from the seed-unloading port; M_3 is the number of times 0 seeds are discharged from the seed-unloading port.

Since it is not possible to measure the spacing between seeding grains during the simulation, the design plan calls for using the Grid Bin Group function of the EDEM Selection post-processing module to set up a monitoring area at the seed-unloading port after the simulation is over. This will facilitate the quantification of scoops discharging 0, 1, 2, or more seeds from the seed-unloading port. The data will be exported as illustrated in Figure 17, with each group consisting of 150 seed scoops, and each test group will be repeated three times to derive the average value as the test results.

5.3.2 Effect of U-hole diameter on test metrics

The diameter of the hole in the seed metering spoon influences the efficacy of the seed metering device in acquiring an individual seed during the filling process. The simulation experiment was done with a U-hole depth of 1.78 mm and a seed scoop tilted at a 13° angle to see how the U-hole diameter affected how well the seed metering device worked. We looked at the device's seed discharge for U-hole diameters of 2.06, 2.27, 2.48, 2.69, and 2.90 mm. The results are shown in Figure 18.

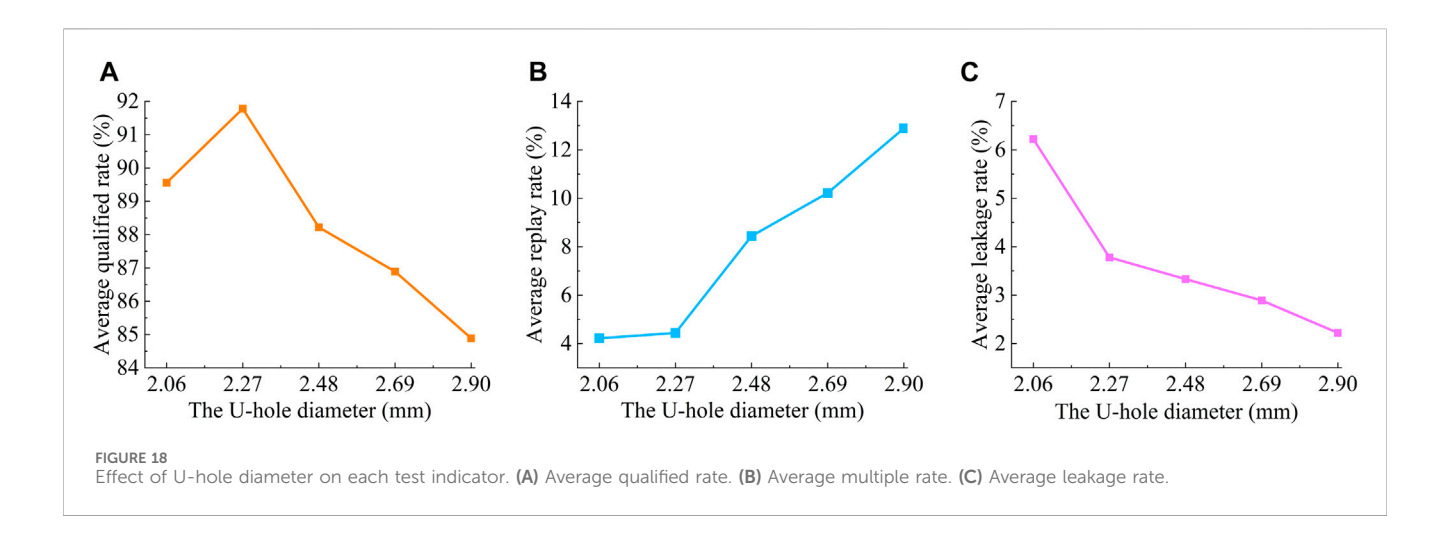
As seen from Figure 18, as the U-hole diameter increases, the seed metering device's qualification rate first goes up and then down, while the play rate steadily goes up and the leakage rate steadily goes down. During seed filling, if the hole opening is excessively small relative to the diameter of the narrower seeds, the hole wall obstructs their entry, leading to an increased leakage rate and a decreased

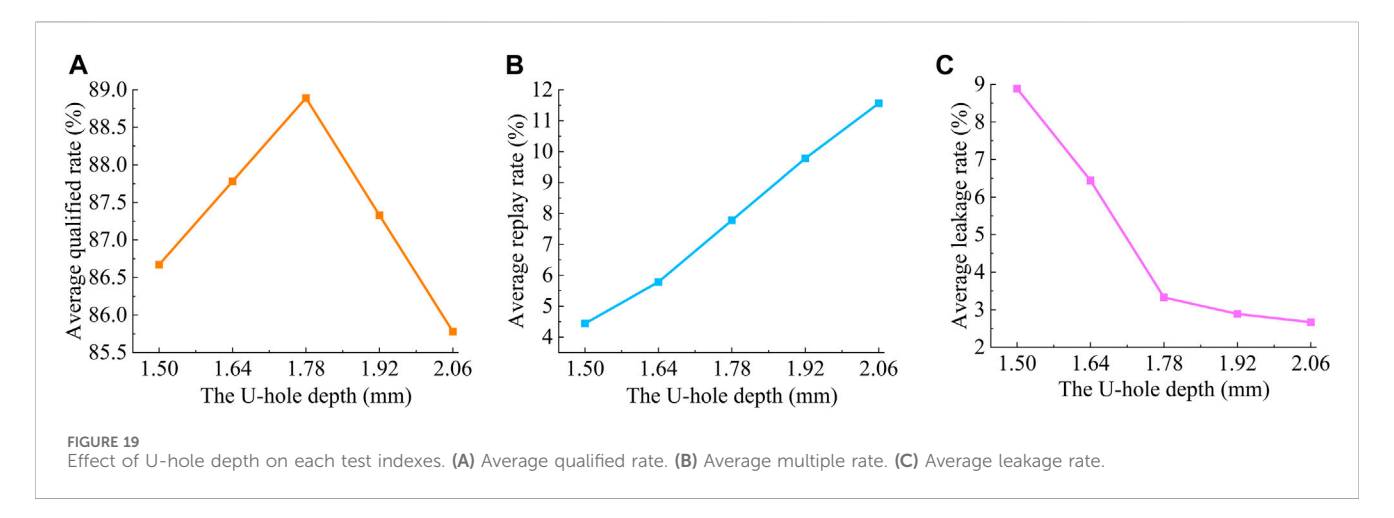
multiple rate. Conversely, if the hole diameter is too large, the volume of the hole increases, allowing multiple seeds to enter, which reduces the leakage rate and increases the multiple rate. When the U-hole diameter measured 2.27 mm, the maximum qualification rate reached 91.78%. The U-hole diameter was established to range from 2.06 to 2.48 mm, taking into account the interaction of factors in subsequent testing.

5.3.3 Effect of U-hole depth on test metrics

The depth of the seed spoon hole is a factor that affects the seed discharge efficacy of the seed metering apparatus. An excessively deep hole enhances seed stabilization but may lead to an overabundance of seeds, hence increasing multiple rates. Conversely, an insufficiently deep hole risks seed displacement, resulting in a heightened leakage rate. Based on earlier tests, the U-hole diameter is set at 2.48 mm, and the inclination angle of the seed scoop's apex is set at 13° for the simulation experiment. This is done to see how the U-hole depth affects how well the seed metering device works. The study focuses on U-hole depths of 1.50, 1.64, 1.78, 1.92, and 2.06 mm to see how well the seed metering device works with discharge. Figure 19 displays the test findings.

In Figure 19, you can see that as the U-hole depth increases, the seed distributor's qualification rate first goes up and then down, while the multiple rate goes up and the leakage rate goes down. When the U-hole depth is insufficient, the seeds occupy the limited depth of the hole; a portion of the seed's center of gravity remains outside the hole in the seed spoon, creating an unstable condition. Consequently, under the influence of gravity and centrifugal force, the seeds may slip from the hole, leading to an increased leakage rate and a decreased replanting rate. Conversely, if the hole depth is excessive, the enlarged hole may accommodate multiple seeds. As the depth of the hole increases, its size expands, resulting in a greater number of seeds occupying it, which leads to a reduction in the leakage rate and an increase in the multiple rate. The highest qualification rate was 88.89% at a seeded spoon hole depth of 1.78 mm. The U-hole depth was found to be between 1.64 and 1.92 mm, taking into account how the parameters would interact in later tests.





5.3.4 Effect of the top inclination angle of seed spoon

The degree of inclination at the top of the seed spoon influences the efficacy of seed discharge in cleaning extra seeds from outside the spoon's aperture. The U-hole diameter was set at 2.48 mm, and the U-hole depth was set at 1.78 mm for the simulation test. This was done to see the effect the angle of the seed spoon's tip had on how well the seed metering device worked. The seed metering device's seed discharge performance is looked at inclination angles of 0°, 6.5°, 13°, 19.5°, and 26°. Figure 20 shows the results.

This is shown in Figure 20. As the tilt angle of the seed spoon goes up, the seed dispenser's qualification rate goes up at first and then down, while the multiple rate goes down and the leaky filling rate goes up. If the angle of inclination at the top of the seed spoon is not sharp enough, some seeds inside the opening might get stuck, making it harder for them to fall. This would increase the leakage rate while decreasing the multiple rate. On the other hand, if the inclination angle is too steep, seeds are more likely to fall out of the aperture, which lowers the multiple rate and raises the leakage rate. The optimal qualification rate of 88.67% was attained with a seed spoon inclination angle of 15°. Considering the inter-actions among the components in the succeeding experiments, the inclination angle of the top of the seed spoon was established to be between 6.5° and 19.5°.

5.4 Quadratic regression orthogonal rotation combination test

5.4.1 Test methods

The optimal ranges for the U-hole diameter, U-hole depth, and the tilt angle of the spoon's apex were determined by analysing the outcomes of the one-factor simulation test on the critical structural parameters of the seed displacement spoon. This study examines how the structural parameters of the seed spoon influence the efficacy of the seed metering device, utilizing the qualifying rate Y_1 , the multiple rates Y_2 , and the leakage rate Y_3 as experimental indicators to identify optimal structural parameters. The Centre-Composite Response Surface Optimization approach accomplishes this with a three-factor, five-level quadratic regression orthogonal rotating combination simulation test. Table 3 displays the experimental factors.

5.4.2 Test results and analysis

The EDEM-based quadratic regression orthogonal rotation combination simulation test program and test results are shown in Table 4. To further analyze the influence law of each test factor and its interaction on the test indexes, regression model ANOVA of qualified rate, multiple rate, and leakage rate of

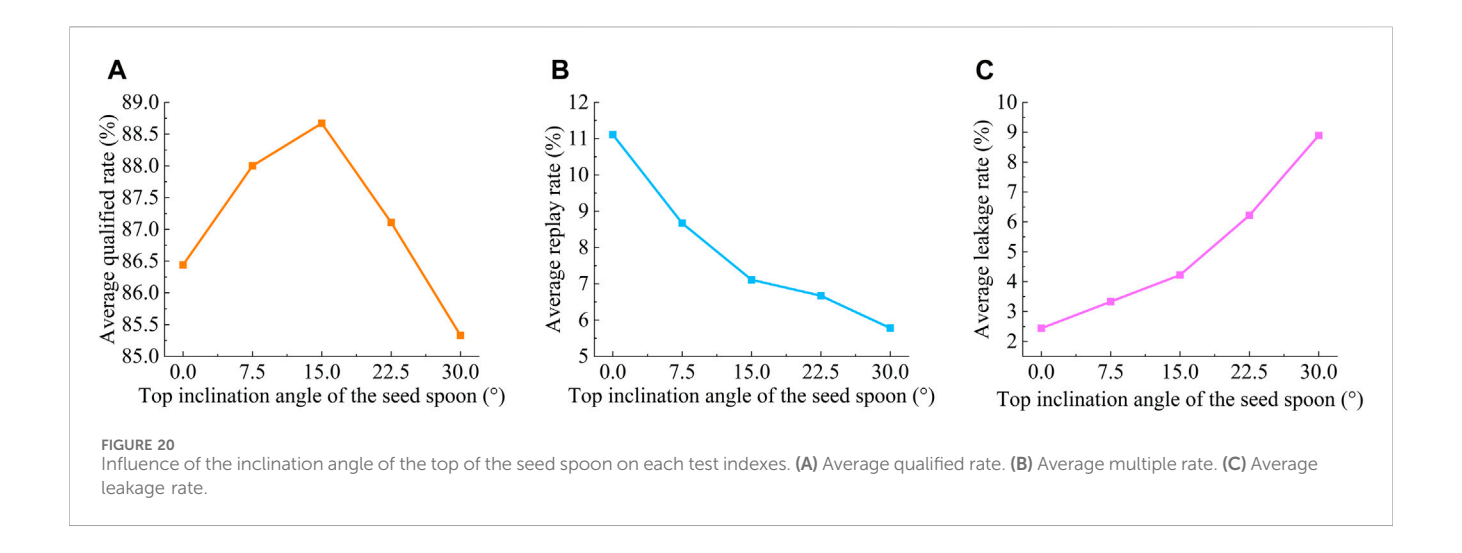


TABLE 3 Test factor code.

Code	Experimental factors								
	U-hole diameter X ₁ /mm	U-hole depth X ₂ /mm	Top inclination angle of seed spoon $X_3/^\circ$						
1.682	2.48	1.92	19.5						
1	2.39	1.86	18.16						
0	2.27	1.78	14						
-1	2.15	1.70	9.14						
-1.682	2.06	1.64	6.5						

simulation test results using Design-Expert 13.0.15 software. The results of the regression model ANOVA and significance test are shown in Table 5.

Table 5 demonstrates that the significance test findings of the regression model for the qualifying rate Y_1 , multiple rate Y_2 , and leakage rate Y_3 are all very significant ($P \le 0.01$). The test findings for the misfit component are all insignificant (P > 0.05), indicating that the regression model is appropriately fitted. R2 values exceed 0.92, which can explain more than 92% of the variation in the evaluation indicators. For the qualified rate regression model, X_2 , X_3 , X_1X_3 , X_2X_3 , X_1^2 , X_2^2 , and X_3^2 are highly significant to the equation, X_1 is significant to the equation, and the rest of the terms are not significant to the equation. For the multiple rate regression model, the effects of X_1 , X_2 , X_3 , X_1^2 , X_2^2 , and X_3^2 on the equation are all highly significant, X_2X_3 has a significant effect on the equation, and the rest of the terms are not significant to the equation. For the leakage rate regression model, the effects of X_1, X_1^2, X_1^3, X_1^2 , and X_3^2 on the equation were all highly significant, X_2 , X_3 , and X_2^2 were all significant, and the rest of the terms were significant to the equation.

We got the quadratic regression equation that connects the factors to the qualifying rate Y_1 , the multiple rate Y_2 , and the leakage rate Y_3 by taking out the coefficients of the following factors that do not matter which was calculated by the Equation 20:

$$\begin{cases} Y_1 = +91.88 - 0.23X_1 - 0.44X_2 + 1.43X_3 + 0.50X_1X_3 \\ +0.39X_2X_3 - 1.08X_1^2 - 0.61X_2^2 - 1.16X_3^2 \\ Y_2 = +4.22 + 0.96X_1 + 0.73X_2 - 1.15X_3 - 0.47X_2X_3 \\ +0.79X_1^2 + 0.83X_2^2 + 0.56X_3^2 \\ Y_3 = +3.90 - 0.73X_1 - 0.30X_2 - 0.27X_3 + 0.42X_1X_2 \\ -0.69X_1X_3 + 0.29X_1^2 - 0.22X_2^2 + 0.60X_3^2 \end{cases}$$
(20)

5.4.3 Effect of test factors on test indicators

To look at how test factors affect each test index and how reseeding and omission affect the simulation process, Design-Expert 13.0.15 was used to make Figure 21, which shows a response surface plot showing the important effects of test factor interactions on the qualified rate Y_1 , the multiple rate Y_2 , and the leakage rate Y_3 .

Figure 21a shows how the qualifying rate Y_1 changes when the inclination angle of the seed spoon tip X_3 and the U-hole diameter X_1 interact with each other. Once the tilt angle of the seed spoon is known, the qualification rate goes up at first as the U-hole diameter gets bigger, but then it goes down. As the diameter of the U-hole is fixed, the qualification rate initially increases and subsequently decreases with the rising inclination angle of the seed spoon's apex.

Figure 21b shows how the qualifying rate Y_1 changes when the inclination angle of the seed spoon tip (X_3) and the U-hole depth (X_2) interact with each other. As the inclination angle of the seed spoon's tip is fixed, the qualification rate initially rises and thereafter declines with an increase in U-hole depth. When the depth of the U-hole is fixed, the qualification rate exhibits a pattern of initial

TABLE 4 Test program and test results.

Code	Test factor			Test indexes					
	<i>X</i> ₁	<i>X</i> ₂	<i>X</i> ₃	Qualified rate $Y_1/\%$	Multiple rate $Y_2/\%$	Leakage rate Y ₃ /%			
1	-1	-1	-1	88.89	5.33	5.78			
2	1	-1	-1	88.00	6.89	5.11			
3	-1	1	-1	87.33	8.67	4.00			
4	1	1	-1	85.78	9.33	4.89			
5	-1	-1	1	90.00	3.78	6.22			
6	1	-1	1	91.33	6.00	2.67			
7	-1	1	1	90.22	5.11	4.67			
8	1	1	1	90.44	6.67	2.89			
9	-1.682	0	0	89.56	4.22	6.22			
10	1.682	0	0	88.22	8.44	3.33			
11	0	-1.682	0	90.67	5.78	3.55			
12	0	1.682	0	89.78	7.11	3.11			
13	0	0	-1.682	86.44	7.78	5.78			
14	0	0	1.682	90.89	3.56	5.56			
15	0	0	0	91.78	4.44	3.78			
16	0	0	0	92.00	4.22	3.78			
17	0	0	0	92.22	3.78	4.00			
18	0	0	0	92.22	3.56	4.22			
19	0	0	0	91.78	4.44	3.78			
20	0	0	0	91.56	4.22	4.22			
21	0	0	0	91.78	5.11	3.11			
22	0	0	0	92.00	4.00	4.00			
23	0	0	0	91.56	4.22	4.22			

increase followed by a decrease as the inclination angle of the seed spoon's apex rises.

Figure 21c shows what happens to the multiple rate Y_2 when the tilt angle of the seed spoon tip (X_3) and the depth of the U-hole (X_2) interact. As the inclination angle of the seed spoon's tip is fixed, the play rate initially rises with an increase in the depth of the U-hole. As the depth of the U-hole is established, the play rate generally diminishes with an increase in the inclination angle of the seed spoon's tip.

Figure 21d shows how the relationship between the U-hole depth (X_2) and the U-hole diameter (X_1) affects the rate of leakage (Y_3) . As the depth of the U-hole is fixed, the leakage seeding rate generally diminishes with an increase in its diameter. As the diameter of the U-hole is fixed, the rate of leakage seeding generally diminishes with an increase in the depth of the U-hole.

In Figure 21e, you can see how the leakage rate Y_3 changes when the angle X_3 of the seed spoon tip and the diameter X_1 of the U-hole interact. As the inclination angle of the seed spoon's tip remains constant, the leakage rate generally diminishes with an increase in the U-hole diameter. As the diameter of the U-hole is fixed, the leakage rate generally escalates with an increase in the inclination angle of the top of the seed spoon.

Response surface analysis shows that as the U-hole's diameter and depth increase, so does its volume. This makes it easier for the seed to fill the hole and keeps it stable. This leads to a reduction in the leakage rate and an improvement in the qualified rate. However, when the hole volume becomes excessively large, it causes repeated seed filling, making it difficult for excess seeds to escape, raising the replanting rate and diminishing the qualified rate. As the tilt angle of the seed spoon's apex increases, the support force for extra seeds outside the spoon's opening goes down. This enhances the metering device's efficacy in seed clearance, reducing the multiple rates and increasing the qualifying rate. However, suppose the inclination angle becomes excessively large. In that case, the target seeds are prone to slipping from the designated hole, increasing the leakage rate and decreasing the qualified rate.

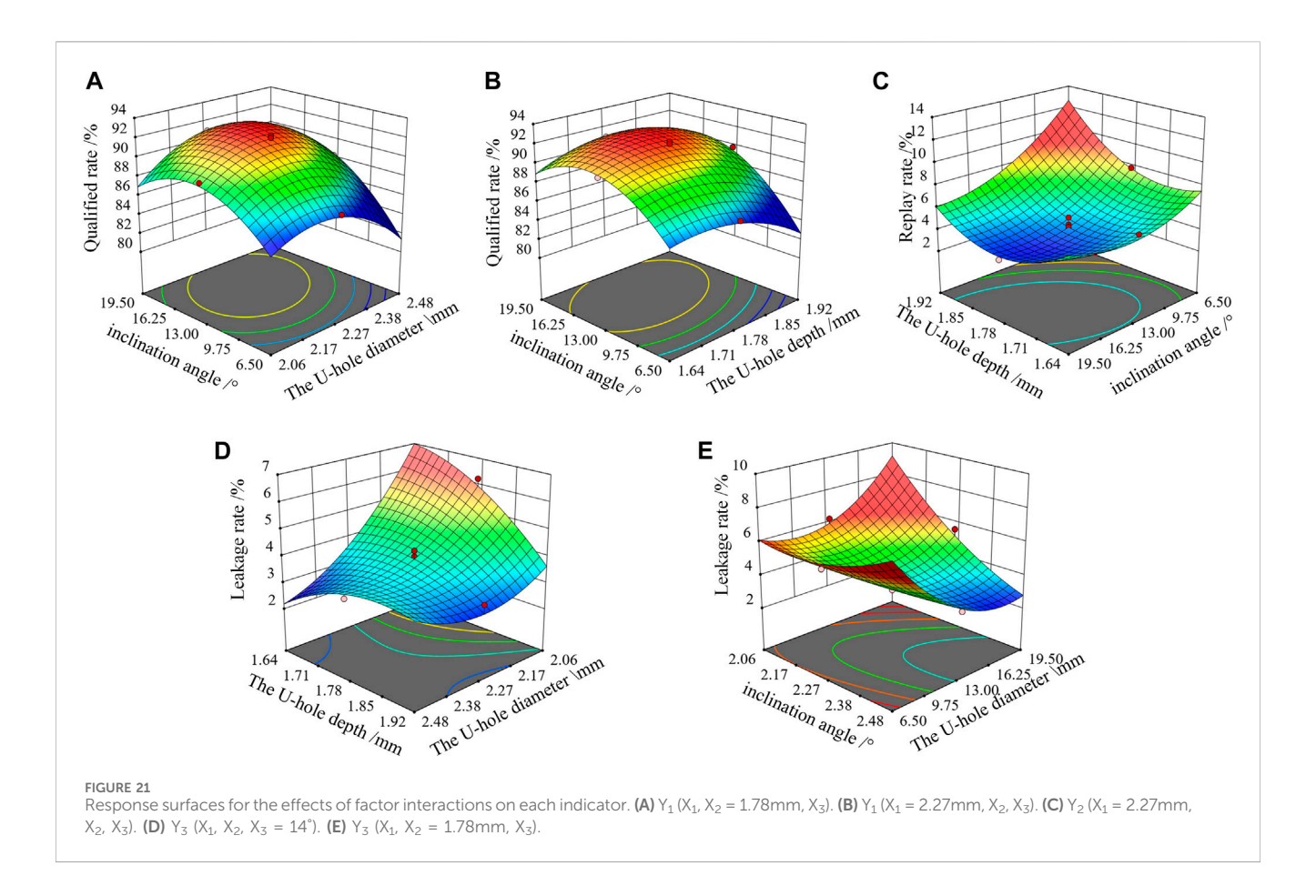
5.4.4 Optimal parameter optimization

A quadratic regression model is created to obtain the optimal combination of structural parameters of the seed spoon. The optimization goals are high qualification rates, low leakage, and low reseeding rates. This model will facilitate multi-objective optimization and solutions, incorporating the objective function

TABLE 5 Regression equations analysis of variance.

Source of	Qualified rate Y ₁			Multiple rate Y ₂			Leakage rate Y₃					
variance	Square sum	Degrees of freedom	F	Р	Square sum	Degrees of freedom	F	Р	Square sum	Degrees of freedom	F	Р
Mould	79.66	9	95.02	<0.0001**	65.85	9	25.32	<0.0001**	22.69	9	17.49	<0.0001**
X_1	0.72	1	7.77	0.0154*	12.56	1	43.47	<0.0001**	7.28	1	50.49	<0.0001**
X_2	2.59	1	27.80	0.0002**	7.35	1	25.43	0.0002**	1.21	1	8.41	0.0124*
X_3	27.77	1	298.09	<0.0001**	18.18	1	62.92	<0.0001**	1.00	1	6.95	0.0205*
X_1X_2	0.39	1	4.20	0.0611	0.30	1	1.05	0.3236	1.39	1	9.62	0.0084**
X_1X_3	1.99	1	21.36	0.0005**	0.30	1	1.05	0.3236	3.85	1	26.71	0.0002**
X_2X_3	1.21	1	12.98	0.0032**	1.79	1	6.18	0.0273*	0.056	1	0.39	0.5435
X_1^2	18.74	1	198.06	<0.0001**	9.88	1	34.19	<0.0001**	1.31	1	9.09	0.0099**
X_2^2	5.99	1	62.55	<0.0001**	10.93	1	37.81	<0.0001**	0.79	1	5.51	0.0345*
X_3^2	21.58	1	228.38	<0.0001**	4.90	1	16.95	0.0012**	5.79	1	40.17	<0.0001**
Residual	1.21	13			3.76	13			1.87	13		
Incoherent	0.72	5	2.32	0.1393	2.19	5	2.24	0.1490	0.88	5	1.42	0.3150
Inaccuracies	0.49	8			1.57	8			0.99	8		
Aggregate	80.87	22			69.61	22			24.56	22		

Note: **Very significant (P < 0.01), *Significant ($0.01 \le P < 0.05$), indicates not significant (P > 0.05).



and constraints based on the boundary conditions for each factor's value which was calculated by the Equation 21:

$$\begin{cases} \max Y_1 \\ \min Y_2 \\ \min Y_3 \end{cases}$$
s.t.
$$\begin{cases} 2.06 \text{mm} \le X_1 \le 2.48 \text{mm} \\ 1.64 \text{mm} \le X_1 \le 1.92 \text{mm} \end{cases}$$

$$6.5^{\circ} \le X_1 \le 19.5^{\circ}$$

$$(21)$$

The Design-Expert software's constraints and optimization solution function yielded optimal seed discharge performance with a U-hole diameter of 2.32 mm and a U-hole depth of 1.76 mm. The inclination angle of the seed spoon's apex was 15.34°, with a seed discharge qualification rate of 92.22%, a multiple rate of 4.21%, and a leakage rate of 3.57%. To make sure the optimization data was correct, three sets of simulation tests were run under the same conditions. The average of the results showed that the seed metering device had a qualified rate of 92.67%, a multiple rate of 4%, and a leakage rate of 3.33%. The results were in line with what the software optimization predicted, which showed that the response surface optimization results were correct.

6 Seeding performance tests

6.1 Bench test

6.1.1 Test materials and devices

To ascertain the reliability of the simulation test, the "Chinese Lai Shen" Chinese cabbage seeds were employed as the test

specimens. The test verification occurred on 5 September 2024, at the self-constructed seed discharging test bed within the Intelligent Agricultural Machinery and Equipment Engineering Laboratory at Harbin Jianqiao College. The seed metering device was fabricated using 3D printing technology with PLA material based on the parameters adjusted by simulation. To enhance the visibility of seed movement within the seed metering apparatus, the front casing was fabricated from an acrylic plate. The experimental configuration is depicted in Figure 22. A conveyor belt is used to simulate the forward speed of the seeder during sowing, and a custom sand-laying apparatus spreads quartz sand to look like field soil. This makes sure that seeds land on the conveyor belt without rolling back. The seed dispenser is stationary during the test and powered by a DC brushless motor, with its rotational speed regulated by the controller. The testing detection apparatus employs a proprietary picture recognition technique. As the seeds descend onto the quartz sand and are conveyed to the monitoring area via the conveyor belt, the system obtains the seeds' coordinates by capturing their images with the Open MV camera. It then computes the difference between the current seeds' coordinates and those of the preceding seeds to determine the inter-seed spacing. A high-speed camera captures and records the complete motion of the seeds within the seed metering apparatus.

6.1.2 Test materials and devices

Since the seed distributor employs an electrically driven and controlled system, the rotational speed of the seed groove will

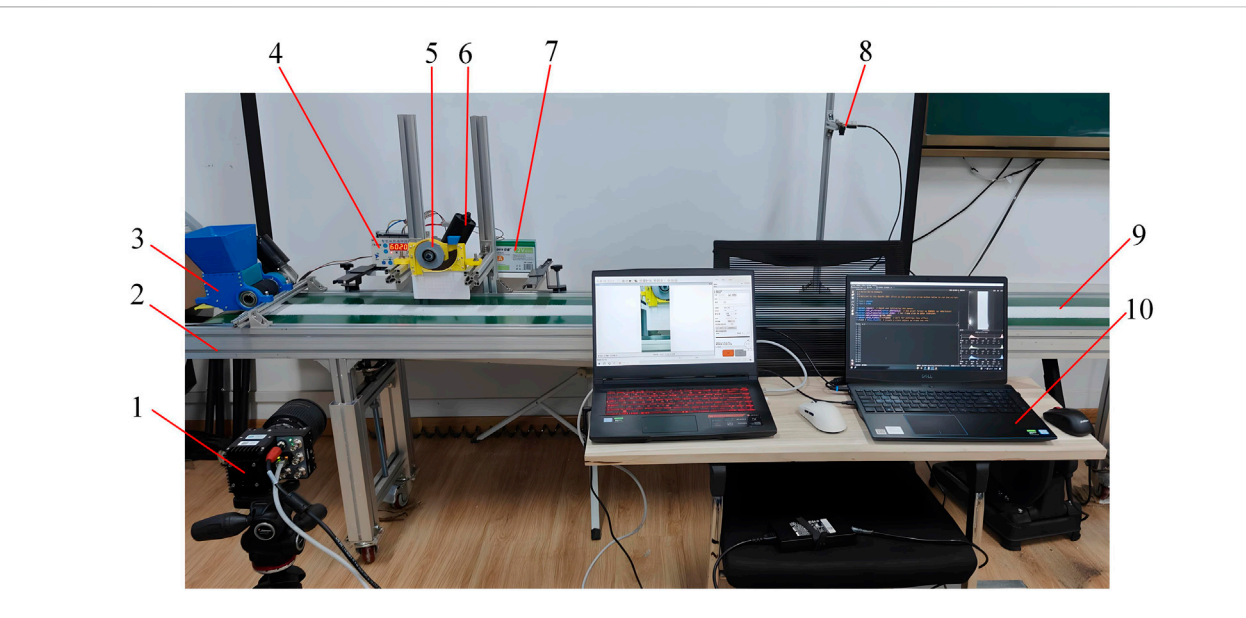


FIGURE 22
Seed Dispenser Bench Test. 1. High-speed photography 2. Conveyor belt 3. Sand spreader 4. Seeding Controller sand 5. Seed metering device 6.
Brushless DC motor 7. batteries 8. Open MV camera 9. Quartz sand 10. Notebook computers.

fluctuate within a certain range during operation as the forward speed of the push-type seeder changes. To further demonstrate the seed distributor's adaptability to different operating speeds of the implement, performance tests were conducted under various seed distribution rotational speeds. The spacing between Chinese cabbage seeds (B_b) was set at 30 cm. The conveyor belt speed ranged from 0.4 to 1.2 m/s, corresponding to seed groove rotational speeds (n) as follows:

$$n = \frac{60V_m}{SZ} \tag{22}$$

Where: V_m is the Seeder Forward Speed, m/s; S is the Spacing for Chinese cabbage seeds, m; Z is the Number of seed scoops at the circumferential position of the seed groove.

According to Formula 22, the seed groove rotational speed was calculated to be 10-30 r/min. Five different working speeds of 0.4, 0.6, 0.8, 1.0, and 1.2 m/s were selected, corresponding to seed groove rotational speeds of 10, 15, 20, 25, and 30 r/min, respectively, for bench testing verification. The performance of the seed distributor was evaluated by measuring the seed spacing on the quartz strip. Following GB/T 6973-2005 "Test Methods for Single-Seed (Precision) Seeders," The assessment employs the test methodology for single seeders, utilizing pass index G (%), reseeding index J (%), and leakage index K (%) used as indicators for the bench test. S represents the theoretical plant spacing, and S_1 denotes the measured plant spacing. Based on cabbage seeding a gronomic requirements in Northeast China, ${\cal S}$ is set to 30 cm. When $0.5S < S_1 \le 1.5S$, the result is considered qualified; $S_1 \le 0.5S$ indicates double seeding; $S_1 > 1.5S$ indicates skipped seeding, as shown in Figure 23. Each test measures the spacing of 150 seeds, with three repetitions averaged. The calculation formula for the test indicators is obtained from Equation 23:

$$G = \frac{\sum n_i (X_i \in \{>0.5 \sim \le 1.5\})}{N} \times 100\%$$

$$J = \frac{\sum n_i (X_i \in \{0 \sim \le 0.5\})}{N} \times 100\%$$

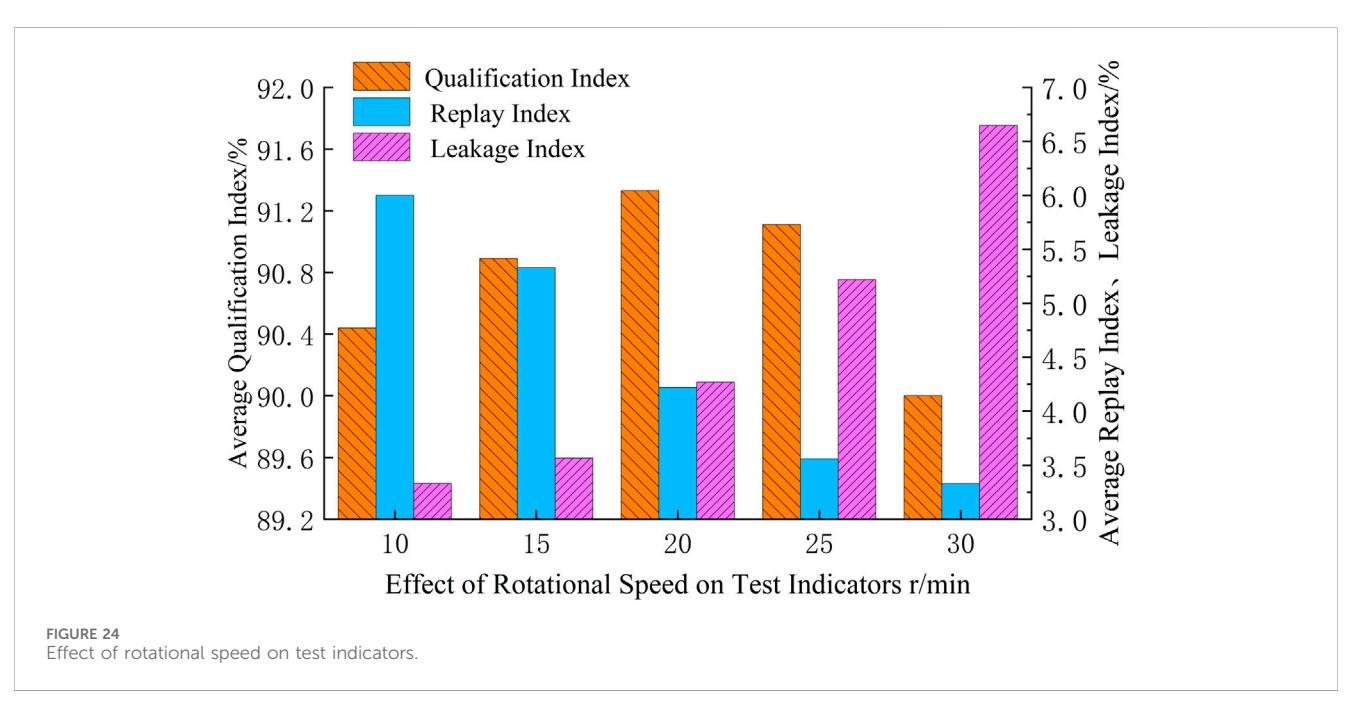
$$K = \frac{\sum n_i (X_i \in \{>1.5 \sim +\infty\})}{N} \times 100\%$$
(23)

Where: Σ_{ni} is the number of occurrences; X_i is the ratio of measured to theoretical seed spacing; and N is the total number of segments.

As shown in Figure 24, with increasing seed groove rotational speed, the qualified index first rises then falls, the re-seeding index continues to decrease, while the skipped-seed index continues to increase. This occurs because the centrifugal force of the seed groove increases with rotational speed, making it difficult for seeds to be stably filled into the seed scoop-shaped holes and causing them to be easily flung out of the holes. Consequently, the skipped-seed index rises while the qualified index decreases.

When the rotational speed of the seed metering device is at 20r/ min, the qualified index of seed dispensing in the bench test is 91.33%, the reseeding index is 4.89%, and the leakage index is 3.78%. Comparison and analysis of the results of the bench test and the simulation test yielded error values of 1.34%, 0.89%, and 0.45%, respectively, which indicate that the results of the bench and the simulation test are consistent, and the simulation test is validated to have certain-liability of the simulation test. The accuracy of the simulation results was verified. When the seed groove speed ranged from 10 to 30 r/min (corresponding to machine operating speeds of 0.4-1.2 m/s), the seed placement qualification index remained no less than 90%, the double-seeding index did not exceed 7%, and the skipped-seed index did not exceed 4%. All test metrics exceeded the operational performance requirements specified in JB/T 10293-2013 "Technical Conditions for Single-Seed (Precision) Seeders" for theoretical seed spacing (plant spacing) within $20 < S \le 30$ mm $(G \ge 80\%, J \le 15\%, K \le 8\%)$. This demonstrates that the seed





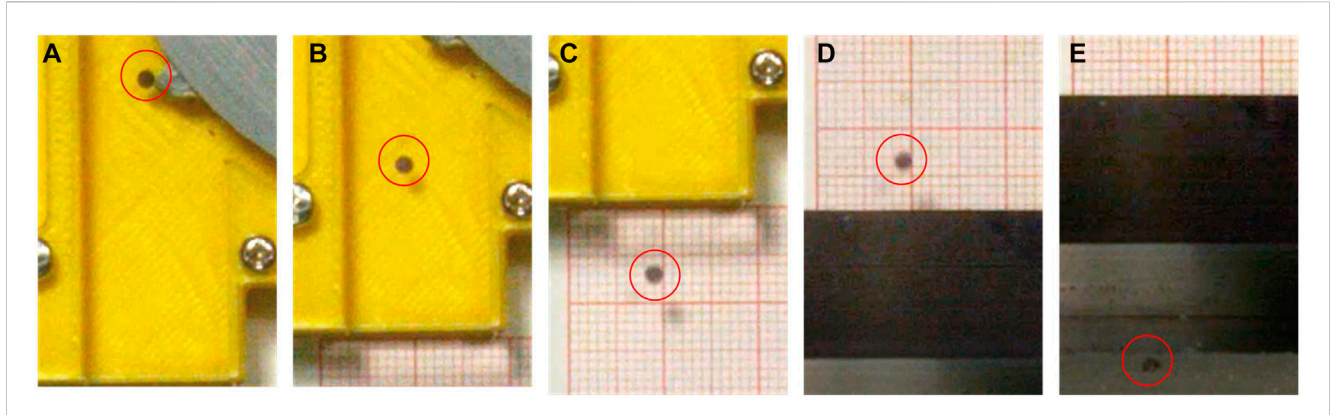


FIGURE 25
Field sowing test. (A) 0s. (B) 0.5s. (C) 0.15s. (D) 0.37s. (E) 0.50s.



FIGURE 26
Field sowing test. (A) Field sowing trials. (B) Chinese cabbage seedling emergence effect.

distributor's seeding performance meets the agronomic requirements for precision direct seeding of Chinese cabbage.

At the same time, a high-speed camera was used to test the seed metering device performance of the seed discharger, as shown in Figure 25, to observe whether the seeds could drop in a straight line, and the straight line seed drop rate Y_4 was taken as the test index. The calculation formula is shown in Equation 24.

$$Y_4 = \frac{m_4}{M_1} \times 100\% \tag{24}$$

Where: m_4 the number of seeds that can drop in a straight line (i.e., without touching the wall or changing their trajectory in the process of falling seeds); M_1 row of seeds in the hole of the number of seeds for the number of one seed spoon.

According to the test results, a linear seed drop rate of 90.18% was achieved, indicating superior seed discharge performance of the metering device.

6.1.3 Seed breakage rate test

A bench test was done to see if the seed metering device's working method reduces seed damage. The test compared the seed metering device to a standard horizontal disc seed metering device (Zhang et al., 2024b). The test conditions were standardized, and at the conclusion of the test, seeds that fell onto quartz sand were collected. By observing the seeds for any visible damage, the breakage rate of the seed metering device denoted as φ_s , was determined. The calculation formula is shown in Equation 25.

$$\phi_s = \frac{e_s}{E_s} \times 100\% \tag{25}$$

Where: e_s is the number of visibly damaged seeds individuals; E_s is the total number of seeds after collection, individuals.

The calculated average seed breakage rates were 0.22% and 1.14%, respectively. The results were in line with the agricultural standard that says mechanical seed meters should have a seed

breakage rate of \leq 1.5% (Dun et al., 2024b); however, there was an 80.70% difference in error between the two. The results indicated that the groove and spoon dischargers could significantly diminish the seed breakage rate.

6.2 Field test

On 10 September 2024, at the experimental field of Harbin Cambridge College in Heilongjiang Province, the seeder's performance was tested by planting seeds in the field. The ideal parameter combination is shown in Figure 26a. Prior to the test, the test field was mildly tilled using a rotary tiller to prepare the soil for the direct seeding of Chinese cabbage, achieving a soil firmness of 12.4 KPa and a moisture content of 12.30%. The seed measuring tool is attached to a small planter that can be used by hand. A 12V DC brushless motor makes it easier for the tool to turn, and a custom Beidou navigation seeding controller controls it. In the operation process, the use of the Beidou navigation system for real-time monitoring of the operating speed of the seeder. The system evaluates the machine's actual walking speed and subsequently regulates the seeding speed to ensure alignment with the predetermined plant spacing of 0.3 m for Chinese cabbage. The operational speed of the hand-push planter varies between 0.4 and 1.2 m/s, corresponding to a seeding groove rotational speed of 10–30 r/ min. The test was conducted over a distance of 10 m and repeated three times.

Fifteen days post-sowing, the growth of Chinese cabbage seedlings was assessed, as illustrated in Figure 26B. Utilizing a steel plate ruler, continuous measurements of the inter-plant spacing within a sampling area of 3 * 10 m were conducted. The results indicated that the field seeding qualification index of the seed dispenser was 89.90%, the multiple index is 6.06%, leakage index is 4.04%. The results meet the requirements of the national standard JB/T 10293-2013, which says that the qualification index must be at least 80%, the multiple index must be at least 15%, and the leakage index must be at least 8%. This study offers a foundational basis for the design and investigation of mechanical precision seeders for Chinese cabbage.

7 Conclude

- 1. Aiming at the problems of small grain size, easy to break, light quality of Chinese cabbage seeds, which cause difficulty in seed filling, easy to injure seeds and poor uniformity of seed-unloading in sowing operation, design a U-hole Chinese cabbage groove-spoon type precision seed metering device with guide seed unloading grooves, and through theoretical calculations and kinematics analyses, determine the structural parameters of the key components: the number of seed scoops is 8, the depth of guide seed unloading groove is 0.3 mm, the depth of seed unloading grooves is 0.43 mm, and the diameter of seeding grooves is 80 mm.
- 2. Do a theoretical analysis to find the most important factors that affect how well the seeds are discharged. These factors are the U-hole diameter, the U-hole depth, and the seed spoon's tilt. To do a single-factor test and a quadratic regression orthogonal rotary combination test, use the qualified rate, the multiple

rates, and the leakage rate as test indicators. Use Design-Expert 13.0.5 to look at the test results, create a mathematical model that connects the qualified rate, multiple rates, leakage rate, and test indices, run multi-objective optimization on the test results, and find the best set of parameters for a U-hole diameter of 2.32 mm, a U-hole depth of 1.76 mm, and a spoon tilt angle of 15.34°. At this configuration, the qualified rate of the seed, the multiple rate, and the leakage rate are 92.22%, 4.21%, and 3.57%, Through multiple simulation tests of the optimal parameter combinations, the average values confirmed that the qualified seeding rate, multiplication rate, and leakage rate were 92.67%, 4%, and 3.33%, respectively. These numbers were in line with what the software optimization predicted. This indicates that the results of the response surface optimization possess a degree of accuracy.

- 3. Empirical validation of the best parameter configuration. It shows that the bench seed filling performance test had a seed arrangement qualification index of 91.33%, a multiple index of 4.89%, a leakage index of 3.78%, and errors of 1.34%, 0.89%, and 0.45% compared to the simulation test results. The consistency between the bench test and the simulation test validates the reliability of the simulation. Field test results reveal that the machine's seed dispenser operates at a forward speed of 0.4–1.2 m/s, with a seed dispensing qualification index of 89.90%, a re-seeding index of 6.06%, and a leakage index of 4.04%, thereby satisfying the seeding performance requirements for Chinese cabbage.
- 4. Groove-spoon Type Precision seed metering device seed discharge performance bench test and with the tradition-al horizontal disc seed metering device breakage rate bench comparison test to get the Groove-spoon Type Precision seed metering device straight line seed drop rate of 90.18%, breakage rate of 0.22%, the traditional horizontal seed metering device breakage rate of 1.14%, the two breakage rate of the relative error of 80.70%, the test results show that the groove and spoon type precision seed discharger can be in the process of working test results show that the Groove-spoon Type Precision seed metering device can effectively reduce the damage to the seeds and improve the uniformity of seed discharge in the working process.

Data availability statement

The original contributions presented in the study are included in the article/Supplementary Material, further inquiries can be directed to the corresponding author.

Author contributions

GD: Conceptualization, Funding acquisition, Methodology, Project administration, Resources, Supervision, Writing – review and editing. CM: Conceptualization, Data curation, Formal Analysis, Investigation, Visualization, Writing – original draft. CZ: Data curation, Software, Validation, Writing – review and editing. XJ: Investigation, Validation, Visualization, Writing – review and editing. YH: Software, Writing – review and editing.

Funding

The authors declare that financial support was received for the research and/or publication of this article. This research was funded by Harbin Cambridge University Key Scientific Research Application Research Project, grant number JQZKY2022021, and Heilongjiang Province Natural Science Foundation of China, grant number LH2023E025.

Conflict of interest

The authors declare that the research was conducted in the absence of any commercial or financial relationships that could be construed as a potential conflict of interest.

Generative AI statement

The authors declare that no Generative AI was used in the creation of this manuscript.

References

Chen, Z., Xue, D., Guan, W., Guo, J., and Liu, Z. (2023). Performance optimization of a spoon precision seed metering device based on a maize seed assembly model and discrete element method. *Processes* 11 (11), 3076. doi:10.3390/pr11113076

China Academy of Agricultural Mechanization Sciences (2007). Agricultural machinery design manual. Beijing: China Agricultural Science and Technology Press.

Ding, L., Yuan, Y., Dou, Y., Li, C., He, Z., Guo, G., et al. (2024). Design and experiment of air-Suction Maize seed metering device with Auxiliary Guide. *Agriculture* 14 (2), 169. doi:10.3390/agriculture14020169

Dong, J., Zhang, S., Zheng, Z., Wu, J., Huang, Y., and Gao, X. (2024). Development of a novel perforated type precision metering device for efficient and cleaner production of maize. *J. Clean. Prod.* 443, 140928. doi:10.1016/j.jclepro.2024.140928

Du, X., Liu, C., Jiang, M., Zhang, F., Yuan, H., and Yang, H. (2019). Design and experiment of self-disturbance inner-filling cell groove maize precision seed metering device. *Trans. Chin. Soc. Agric. Eng. Trans. CSAE* 35 (13), 23–34.

Dun, G., Liu, W., Mao, N., Wu, X., Ji, W., and Ma, H. (2023). Optimization design and experiment of alternate post changing seed metering device for soybean plot breeding. *J. Jilin Univ. Technol. Ed.* 53 (1), 285–296.

Dun, G., Zhang, C., Ji, X., Meng, Q., Sheng, Q., and Wang, L. (2024). Simulation parameter calibration and Test of Pak Choi seeds based on discrete element method. *INMATEH Agric. Eng.* 73 (2), 63–72.

Dun, G., Guo, N., Ji, X., Li, X., and Wang, L. (2024). Design and experiment of a spoon type precision seeder for hanging seeds on the side of carrots. *J. Agric. Mach.* 55 (05), 77–86+97.

Fang, L., Cao, C., Meng, K., and Cao, J. (2022). Design and experiment of groove seed metering device with guide ring groove combining U-hole for Radix peucedani. *J. Agric. Mach.* 53 (04), 21–32+51.

Gao, X., Cui, T., Zhou, Z., Yu, Y., Xu, Y., Zhang, D., et al. (2021). DEM study of particle motion in novel high-speed seed metering device. *Adv. Powder Technol.* 32, 1438–1449. doi:10.1016/j.apt.2021.03.002

GBT (2005). Test method for single seed (precision) seeder.

JBT (2013). Technical conditions for single seed (precision) seeder.

Li, Y. H., Zhang, Z. L., and Ti, H. (2020). Design and experiment of groove spoon type garlic single seed picking device. *J. Agric. Mach.* 51 (03), 61–68.

Li, H., Zhao, W., Shi, L., Dai, F., Rao, G., and Wang, Z. (2024a). Design and Test of seed Ladle tongue type flax precision burrow planter. *Trans. Chin. Soc. Agric. Mach.* 55 (3), 85–95.

Li, Y., Zhao, S., Yang, F., Liu, P., Li, B., Song, Q., et al. (2024b). Research on the flexible gradual seed-cleaning method of the brush-type single-seed soybean planter. *Agriculture* 14 (3), 399. doi:10.3390/agriculture14030399

Any alternative text (alt text) provided alongside figures in this article has been generated by Frontiers with the support of artificial intelligence and reasonable efforts have been made to ensure accuracy, including review by the authors wherever possible. If you identify any issues, please contact us.

Publisher's note

All claims expressed in this article are solely those of the authors and do not necessarily represent those of their affiliated organizations, or those of the publisher, the editors and the reviewers. Any product that may be evaluated in this article, or claim that may be made by its manufacturer, is not guaranteed or endorsed by the publisher.

Supplementary material

The Supplementary Material for this article can be found online at: https://www.frontiersin.org/articles/10.3389/fmech.2025. 1704283/full#supplementary-material

Liu, T., He, R., Lu, J., Zou, Y., and Zhao, M. (2016). "Simulation and experiment of seeding performance of nest eye groove rapeseed planter based on EDEM," 37. Guangzhou, Guangdong, China: South China Agricultural University, 126–132.

Ma, J., Sun, S., Wang, J., Hu, B., Luo, X., and Xu, X. (2024). An experimental analysis of the seed-filling mechanism of maize-precision hole-planter clamping. *Agriculture* 14 (3), 398. doi:10.3390/agriculture14030398

Su, W., Chen, Z. W., Lai, Q. H., Jia, G. X., Lu, Q., and Tian, B. N. (2022). Design and Test of Groove-spoon Type Precision seed metering device for Chinese Herbal Medicine Pinellia ternate. *Trans. Chin. Soc. Agric. Mach.* 53 (09), 60–71.

Sun, W., Yi, S., Qi, H., Wang, S., Li, Y., and Dai, Z. (2024). Design and experiment of twin discs intertwined air-pressure high-speed precision seed metering device for maize delta-row dense plantings. *Trans. Chin. Soc. Agric. Mach.* 55 (10), 168–179.

Wang, S., Lu, M., Liu, X., Ji, J., and Chen, P. (2022). Calibration and analysis of discrete element simulation parameters of Chinese cabbage seeds. $PLoS\ One\ 24$ (6).

Wang, Q., Han, D., Chen, L., Huang, Y., Li, W., and Tang, C. (2024). Simulation And Optimization Of The Spoon-Groove Type Maize Precision Seed Metering Device Based On Vibration. *INMATEH Agric. Eng.*

Xu, J., Cai, Z. S., Zhang, G. S., and Shen, P. (2019). Optimization study on the picking spoon of tilted disc spoon soybean seeder based on discrete element method. *Jiangsu Agric. Sci.* 47 (4), 192–196.

Yang, Y., Cui, Z., Gao, Q., Guan, C., Liu, X., and Chen, Y. (2020). The current situation and development suggestions of mechanized production of Chinese cabbage in China, 11. Haidian, Beijing, China: Chinese Vegetables, 9–16.

Yao, M. (2024). Planting and pest control methods of Chinese cabbage. $Agric.\ Technol.\ Equip.\ 10,\ 148-149.$

Zhang, Q., Yu, Q., Wang, L., Liao, Y., Wang, D., and Liao, Q. (2020). Design and experiment of scoop-type precision hole metering device for rapeseed. *Trans. Chin. Soc. Agric. Mach.* 51 (6), 47–54.

Zhang, R., Liu, H., Wei, G., Zhou, J., Shi, S., Li, H., et al. (2023). Design and test of key components of scoop type precision sorghum seed metering device. *J. Agric. Mech. Res.* 45 (12), 215–219.

Zhang, H., Han, X., Yang, H., Chen, X., Zhao, G., Sun, J., et al. (2024). Calibrating and simulating contact parameters of the discrete element for apple particles. *Trans. Chin. Soc. Agric. Eng.* 40 (12), 66–76.

Zhang, C., Meng, Q., Dun, G., Ji, X., Sheng, Q., and Hou, Z. (2024). Design and Test of horizontal disc pakchoi precision seed metering device. *For. Mach. and Woodwork. Equip.* 52 (10), 68–74.

Zhou, B., and Qian, W. (2022). Comparative analysis of the contribution rate of influencing factors of open-field cabbage planting income in three provinces in Northeast China. *North. Hortic.* (10), 144–150.